Development of Strut and Tie Model for Squat Shear Wall

FINAL YEAR PROJECT UG-2019

By

SAIFULLAH	NUST2019BSCE322313
ABDUL RAHMAN	NUST2019BSCE284940
WAQAS ALI SHAH	NUST2019BSCE284340
SARDAR JAWAD AHMED	NUST2019BSCE283556

NUST Institute of Civil Engineering (NICE)

School of Civil and Environmental Engineering (SCEE)

National University of Sciences and Technology (NUST) Islamabad, Pakistan

2023

This is to certify that The Final Year Project Titled

Development of Strut and Tie Model for Squat Shear Wall

Submitted by

SAIFULLAH	NUST2019BSCE322313
ABDUL RAHMAN	NUST2019BSCE284940
WAQAS ALI SHAH	NUST2019BSCE284340
SARDAR JAWAD AHMED	NUST2019BSCE283556

Has been accepted towards the requirements for the undergraduate degree in

CIVIL ENGINEERING

_____

Dr. Azam Khan

Assistant Professor

National Institute of Civil Engineering (NICE)

School of Civil and Environmental Engineering (SCEE)

National University of Sciences and Technology (NUST), Islamabad

Pakistan

DECLARATION

We completed the thesis "Development of Strut and Tie Model for Squat Shear Wall" entirely, and we confirm that no other person, institution, or source contributed to the work presented in the thesis. All of the external works cited in the thesis have appropriate references. This thesis is an original work that has not been published or submitted for publication elsewhere.

We assure you that we conducted an in-depth study into the subject and worked on it with honesty and integrity. We accept sole accountability for the thesis's contents. We acknowledge the importance of academic integrity and the consequences of plagiarism. As a result, we have taken steps to make sure that all sources are properly cited and acknowledged.

ACKNOWLEDGEMENTS

We begin by expressing gratitude to ALMIGHTY ALLAH, whose blessings have helped to make our journey throughout NUST possible and easy. We are profoundly grateful for the success we accomplished during this incredible journey. We also recognize the commitment and dedication of our team members, who have worked constantly to achieve our goals and objectives.

We cannot ignore the invaluable contribution of our parents, who have always been our pillars of strength and support. Their unwavering prayers and sacrifices have been instrumental in our success, and we are grateful for their unwavering support.

We would also like to thank our advisor and mentor, Dr. Azam Khan, for his invaluable advice, motivation, and support. His guidance has been invaluable in navigating the final year requirements and completing our research work.

We thank our professors and staff members at NUST for their hard work and dedication in providing us with a wealth of knowledge and resources during our time here. Their continuous efforts have assisted us in progressing and achieving success in our academic endeavors.

Finally, we would like to thank everyone who played a role to our success in some way. We appreciate your encouragement and support, and we look forward to the fresh challenges that await us.

TABLE OF CONTENTS

TABLE OF FIGURES

1. INTRODUCTION

1.1. Shear Wall

A shear wall, according to building codes, is a rigid vertical diaphragm capable of transferring lateral forces from the exterior walls, floors, and roofs to the ground foundation in a direction parallel to their planes. Reinforced concrete walls and vertical trusses are common examples. Lateral forces such as wind, earthquake, uneven settlement loads, and the weight of the structure and occupants can create twisting (torsional) forces powerful enough to tear (shear) a building apart. The shape of the frame can be maintained and rotation at the joints prevented by reinforcing it with a rigid wall placed inside or attached to it. Shear walls are particularly important in earthquake-prone high-rise buildings.

It is important to mention that the use of shear walls in building design is now required by building codes in many countries. This is due to the acceptance of shear walls as critical safety features that provide resistance to lateral loads and prevent buildings from collapsing due to twisting forces generated by wind, earthquake, and uneven settlement loads.

In conclusion, shear walls are critical components in modern building construction because they help to keep buildings from collapsing due to the powerful twisting forces generated by lateral loads. The shape of the frame can be maintained and rotation at the joints prevented by reinforcing it with a rigid wall placed inside or attached to it. Shear walls are especially important in high-rise buildings that are subject to lateral wind and seismic forces. Their incorporation into building design is now widely recognized as an essential safety feature, and many countries' building codes require it.[1]

In addition, the American Concrete Institute (ACI) has issued a code for the design and construction of concrete shear walls. The ACI 318 Building Code Requirements for Structural Concrete specifies design, detailing, and construction guidelines for concrete shear walls.

1.2. Squat Wall

Squat walls, such as parking level walls or basement walls, are commonly used in low-rise construction and lower levels of tall buildings. They are also seen in long walls with window and door openings, which result in wall portions between the openings. These walls are intended to provide sufficient shear strength to promote flexural yielding, which necessitates the use of a model that accounts for nonlinear flexural behavior.

Nonlinear shear responses frequently dominate behavior in low-aspect ratio walls. As a result, the modelling parameters for shear stiffness and strength chosen can have a significant impact on the predicted distribution of member forces and building lateral drift. This emphasizes the significance of accurate modelling in squat wall design.

The above paragraph emphasizes that the design of squat walls requires careful consideration of nonlinear flexural behavior and the selection of appropriate modeling parameters to account for shear stiffness and strength. According to the article, squat walls are commonly used in low-rise and lower levels of tall buildings, but they can also be found in long walls with openings.[2]

Experimental evidence suggests that even relatively slender walls with aspect ratios of three to four exhibit flexural and shear deformation interaction, according to Massone and Wallace (2004). Shear deformations account for approximately 30% and 10% of the lateral displacement in the first story and roof level, respectively. However, how much interaction exists for smaller aspect ratios is unknown. To develop accurate modelling approaches that capture key response features, relatively simple models that consider the interaction of flexure and shear responses are required. While many wall tests have been reported in the literature, the majority of them are concerned with determining wall shear strength and lateral displacement response rather than the relative contributions of flexural and shear deformations to wall lateral displacements. Experiments with extremely detailed instrumentation layouts are required to validate existing modelling approaches and develop new ones.[3]

1.3. Strut and Tie Modeling

Strut-and-tie modelling is a structural engineering method for analyzing and designing complex concrete structures like deep beams, corbels, and transfer girders. It entails creating a simplified model of the structure using struts and ties, which are modelled as tension and compression members, respectively. The strut-and-tie model (STM) is used to calculate the structure's internal forces and stresses, as well as the size and spacing of reinforcement required to ensure its safety and stability.

The structure is divided into a series of nodes or regions in the STM approach, with each node representing a point of load or stress concentration. Struts and ties connect the nodes, representing the flow of forces and stresses within the structure. Compression forces are transferred by struts, while tension forces are transferred by ties. The struts and ties are designed in size and shape to reflect the anticipated forces and stresses in the structure, and they are reinforced as needed to ensure their ability to withstand the anticipated loads.

Strut-and-tie modelling is widely used in the design of reinforced concrete structures, and it is particularly useful for complex structures that are difficult to analyze using traditional methods. The STM approach allows engineers to design structures that are both safe and economical by modelling the complex forces and stresses within the structure in a simple and efficient manner.[4]

Researchers use strut-and-tie models to approximate the internal stresses in the compression and tension regions of concrete elements. These models represent the flow of these stresses with struts and ties. It is critical to select an appropriate strut-and-tie model to accurately capture the strength of reinforced concrete (RC) deep beams. The strut-and-tie mechanism is considered the primary load transfer mechanism in RC deep beams, though truss action may also play a role in load transfer in some cases. The type of load transfer mechanism is determined primarily by the shear span to beam depth (a/d) ratio and the amount of shear reinforcement. For beams with an a/d ratio less than 1.0, regardless of shear reinforcement, a single concrete strut forms to transfer the load to the support. As a result, a strut-and-tie model is appropriate for designing and analyzing such elements.[5]

As shown in Fig. A, a strut-and-tie model (STM) is made up of three types of elements: concrete struts (with or without reinforcement) in compression, ties with or without reinforcement, nodes, and nodal zones. Any strut-and-tie model can fail in one of three ways: The tension tie may fail due to yield or anchorage failure, one of the struts may crush if the stress in the strut exceeds the effective compressive strength of concrete, and a nodal zone may fail if it is stressed beyond the effective compressive strength of concrete.[6]

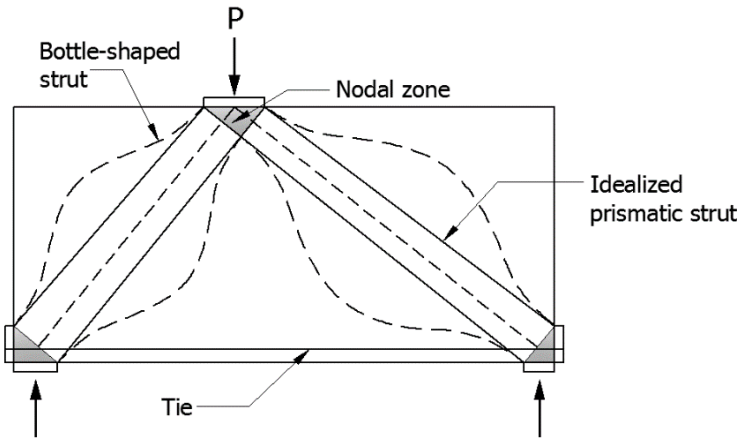

Figure (A) Components of a strut-and-tie model of a deep beam

1.4. Abaqus modelling

Abaqus software comes in handy in visualizing the finite element analysis results, simulating various types of material behavior (including Non-linear and linear elasticity), analysis of different assemblies and mechanical components. It can be used to predict how structures will behave under different loads. It can also be used to determine the strength and stiffness of structures, as well as to identify potential failure points. This information can be used to improve the safety and reliability of structures.

2. LITERATURE REVIEW

2.1. Analyzing Shear Wall Performance and Design Optimization

Reinforced concrete shear walls are popular structural components in buildings and bridges. Seismic failure of these walls can have disastrous consequences, making it critical to accurately identify failure modes. Traditional failure mode identification methods rely on analytical or numerical models, which can be time-consuming and computationally expensive. Recent research has investigated the use of data-driven machine learning techniques to identify failure modes of reinforced concrete shear walls more efficiently.

Machine learning-based approaches for identifying failure modes in reinforced concrete shear walls have been proposed in several studies. Zhang et al. (2020), for example, proposed a convolutional neural network (CNN)-based machine learning model to classify damage patterns in reinforced concrete shear walls. The model identified failure modes with high accuracy, and the authors suggested that it could be used as a tool for post-earthquake damage assessment.[7]

Similarly, Guo et al. (2020) proposed a deep neural network (DNN)-based machine learning approach for identifying the failure modes of reinforced concrete shear walls. The authors used seismic response data collected from physical tests on reinforced concrete shear walls to train the DNN model. The results demonstrated that the model correctly identified the failure modes of the walls.[8]

Wang et al. (2021) used an acceleration response-based support vector machine (SVM) algorithm to identify the failure modes of reinforced concrete shear walls. The authors gathered data from physical tests and used the SVM model to categorize acceleration response signals into various damage categories. The results demonstrated that the SVM model correctly identified the damage patterns on the walls.[11]

Finally, recent research has demonstrated that data-driven machine learning techniques are effective in identifying the failure modes of reinforced concrete shear walls. These methods are

more efficient and accurate than traditional analytical or numerical methods. Future research could concentrate on the development of more robust machine learning models that can be applied to a broader range of structural components and scenarios.

An extensive database created based on the available experiments containing 393 one-story, one-bay reinforced concrete shear walls with rectangular or non-rectangular (barbell or flanged) sections. Specimens with flexural failure (152), flexure-shear failure (96), shear failure (122) and sliding shear failure (23) respectively were examined.[9]

The study assembled eight machine learning models, including Naive Bayes, K-Nearest Neighbors, Decision Tree, Random Forest, AdaBoost, XGBoost, LightGBM, and CatBoost and were evaluated in order to establish the best prediction model.[9]

The proposed Random Forest model had 70% recall and 84% precision in identifying the flexure-shear failure mode for the test set. Critical factors governing the failure mode includes: the aspect ratio, boundary element reinforcement indices, and the wall length-to-thickness ratio.[9]

2.2. Experimental and Analytical Investigation of Shear Strength of Reinforced Concrete Squat Walls under Seismic Loads using STM-based Approaches

A strut-and-tie model (STM) was created to estimate the shear strength of squat shear walls with rectangular, barbell, and flanged cross-sections.[10] The model was developed using two distinct force-transfer mechanisms, namely the diagonal strut and truss mechanisms. The diagonal struts in a squat shear wall transfer shear forces through compressive stresses in concrete, while tension ties carry tensile forces through steel reinforcement.[11] The STM provides a comprehensive approach to predicting the shear strength of various types of squat shear walls by taking these two mechanisms into account.

A dataset of 614 test walls was used to build the model. The peak shear strengths of these test walls were determined through experimental testing. The data obtained served as the foundation for

developing and calibrating the STM. The predicted shear strengths were compared to the peak shear strengths obtained from existing models to validate the model's accuracy.[10] This validation process ensured that the STM could predict the shear strength of squat shear walls with confidence.

Other D-region elements, such as dapped end beams and internal beam-column junctions, might be included to the suggested model. The critical zone near the connection points where shear forces are concentrated is referred to as the D-region.[10] Engineers can improve their understanding of force transfer mechanisms and predict shear strengths more accurately by adapting the STM to these structural elements. This extension enables a more comprehensive analysis of various structural system components, thereby improving the overall design process.

The suggested model's prediction performance and generality were assessed using a ten-fold cross-validation technique. This method entails splitting the dataset into ten subsets, training the model on nine of them, and testing it on the tenth. The model's accuracy and robustness can be evaluated by repeating this process ten times and rotating the subsets. In terms of accuracy, the proposed STM model outperformed both the ACI 318-19 and state-of-the-art models,[10] indicating that it has superior predictive capabilities for estimating the shear strength of squat shear walls.

By developing an interaction correlation between the shear strengths of the diagonal concrete strut and the steel tension tie, the STM model was created. This relationship describes the interaction of compressive and tensile forces within the squat shear wall.[10] Even in the absence of web reinforcement, the model provides a comprehensive representation of shear strength by considering the contributions of both materials. This is especially significant because it enables engineers to analyze and design squat shear walls without the need for additional reinforcement, simplifying the construction process and lowering costs. The STM model provides engineers with a dependable and efficient tool for accurately predicting the shear strength of squat shear walls.

2.3. Mohr-Coulomb Failure Criteria and Significance of the Value of k

The stress distribution factor k is an important design parameter for simply supported deep beams (SSDBs), which are commonly used in buildings and structures. To calculate the stress distribution factor k, the force equilibrium condition must be met, which states that the total vertical forces and

moments acting on the beam must be balanced. Other factors, such as the distribution of horizontal stresses and deformations within the beam can however influence the value of k.[12]

Further from force equilibrium, the value of k is extremely sensitive to the tensile strength of the concrete used in the beam. This is due to the fact that the tensile strength of concrete is difficult to determine accurately in practice and can vary depending on a variety of factors such as the type and quality of materials used, curing conditions, and the age of the concrete. As a result, when calculating the stress distribution factor k, it is critical to account for the uncertainty in the value of concrete tensile strength.[12]

When calculating k, another important factor to consider is the bottom reinforcing component force in the direction of the concrete diagonal strut. For simplicity, this term is frequently overlooked, however it can be important if the strut angle is tiny. In such cases, the component force of the bottom reinforcement can have a significant impact on the value of k, it is crucial to account for the possibility of error in concrete tensile strength values.[12]

The existing model for SSDBs has a limitation in that it does not explicitly account for the softening factor, which is a measure of the decrease in beam stiffness caused by cracking and deformation. The softening factor is a critical parameter that influences the behavior of SSDBs and has a significant impact on the value of k. While the current model implicitly accounts for the softening factor, it is critical to explicitly derive this parameter to ensure accurate SSDB design.[12]

To overcome these constraints, a modified STM (Strut-and-Tie Model) for SSDBs was developed and tested using 233 test specimens from the literature.[12]

Finally, the force equilibrium condition, the uncertain nature of concrete tensile strength, a component of the force of the bottom reinforcement along the path of the concrete diagonal strut, and the softening factor must all be carefully considered when designing SSDBs. This study's modified STM provides a better framework for designing SSDBs and can help ensure the safety and reliability of these structures in practice.[12]

3. AIM

The current study aimed to improve the accuracy of predicting the shear strength of squat walls with an aspect ratio (height to length) of 2 or below, thereby overcoming the limitations of traditional ACI (American Concrete Institute) methods. To accomplish this, we will consider and incorporate various influencing parameters that affect squat wall shear behavior.

Earthquakes are major design concern for structural engineering. Tall buildings are sensitive to wind and earthquake loads and hence slender shear walls are designed to serve the purpose. Pakistan is considered as one of the most seismically active countries in the world. We have observed that not only tall structures, but also small structures are prone to destruction via strong earthquakes as well. Prime locations for high seismic activities are areas closed to mountain regions in Northern and Western regions of Pakistan (Gilgit Baltistan and central region of Baluchistan). The famous October 8, 2005, 7.6 magnitude (Kanamori-1977) resulted in huge human and financial loss. Two to four story establishments were either levelled to ground or developed huge structural cracks. This way the design of Squat Shear walls for smaller building height to length ratio role comes to play.

We have created a numerical model of the squat wall using basic understanding from different researchers' methodologies and validated our model using Abaqus finite element analysis software. Experimental data from previous studies will be used to calibrate and validate the model. This ensures that the numerical model accurately represents the behavior of squat walls in real life.

We will investigate and analyze several influencing parameters with the aim of enhancing the precision of shear strength prediction. Wall thickness, concrete strength, reinforcement ratio, and the presence of shear reinforcement are examples of these parameters. We hope to develop a comprehensive understanding of squat wall shear behavior by taking these parameters and their interactions into account.

To simulate realistic scenarios, the numerical model will be subjected to monotonic loading at various frequencies. The model's response will be compared to experimental data in order to validate its accuracy in predicting shear strength.

The findings of this research will help to advance shear strength prediction methods for squat walls, giving engineers and designers a more reliable tool for structural analysis and design. It will be possible to optimize the design of squat walls by improving accuracy, resulting in safer and more cost-effective structures.

4. RESEARCH METHODOLOGY

4.1. Strut and tie modelling for predicting shear strength of squat shear walls under earthquake loading

4.1.1. Model Novelty

Unlike other equations to determine shear strength of shear walls, our model differs in following ways:

- To determine shear strength, ACI 318 Section 11.5 illustrates equations of slender rectangular walls which underestimates peak shear strength of squat walls.

- When the shear wall height is smaller than that of its horizontal length, the horizontal shear force could be assumed to be transferred directly via diagonal strut, to wall supports. Hence, the resultant shear strength would be more than that of slender shear walls as shear strength is influenced primarily by strut crushing.

- ACI 318 Section 11.5 considers the effect of horizontal web reinforcement only. Whereas Wood (1990) in his research depicted that vertical reinforcement contributes to shear strength of squat walls more in comparison to horizontal web reinforcement [13]. Hence both vertical and horizontal bars were considered in this model.

- For simplicity researchers assume uniform distribution of “stresses at center of the wall”. Therefore, such an assumption is inadequate. Our model inculcates non- uniform stress distribution along the concrete strut. It also accounts for bulging of diagonal concrete strut.

- Softening effect is an effect that occurs in concrete structures when experiences load for longer period, undergoes creep and causes micro cracks in the concrete members. This effect was also incorporated while deriving Mohr - Coulomb failure criteria.

- Normal shear strength derivation doesn't count for boundary element reinforcement contribution, which is found vital at peak shear values. This model accounts for boundary element reinforcement bars as well.

4.1.2. Influencing Parameters

Following influencing parameters were incorporated:

- H/L_w: Height to length ratio (aspect ratio)
- fc: Concrete compressive strength
- $N_c/A_w fc$: Axial load ratio
- A_h and A_v: Area of steel of web horizontal and vertical bars
- A_{be}: Area of steel of boundary elements
- K1: Non-linear strut stress distribution constant

4.1.3. Model derivation

The shear strength of a squat shear wall is primarily provided by the Diagonal strut mechanism and the Truss mechanism.

4.1.4. Assumptions

Following assumptions were made to derive the analytical equation:

- For uniform distribution of vertical bars in rectangular walls, boundary element length is equal to 10% of total length of the wall.
  For concentrated distribution of vertical bars in rectangular walls, boundary element length is equal to "twice the concrete cover plus the length of the region of the concentrated vertical bars", as defined in Section R18.10.6.5 of ACI 318-19.

- The STM approach assumes that the strength of concrete struts governs the shear failure of squat shear walls, and these struts often have lower strength than nodal regions. As a result, this model has ignored the strength of nodal regions and assumed that all forces can be

transferred through the struts. However, when squat shear walls are subjected to high axial loads, nodal regions can fail, particularly those connecting diagonal and truss mechanisms. Thus, it is necessary to consider the strength of nodal zones in these cases and further research is needed on this topic.

- The strut was assumed to be prismatic, having uniform cross section along the length.

- As boundary element confinement effect is found to be negligible, hence it was ignored as well.

- Non-uniform stress distribution was assumed along the strut for simplicity.
  A distribution factor K1 was introduced in the model. To satisfy the equilibrium of forces and moment equilibrium, this constant was utilized and is explained in the next part of the document.

- For diagonal strut mechanism, it was assumed that the axially compressive load is acting on the two points upon the boundary elements. Hence, it is logical to assume that the axial load is participating in diagonal strut mechanism only.

- In strut mechanism, the diagonal strut resists compressive forces Cc and boundary elements vertical bars resist tensile forces T.

- In truss mechanism, the axial rigidity of all truss members was assumed to be equal, (in order to analyze the statically indeterminate Strut and Tie model).

- It is assumed that the squat wall would fail under diagonal compression type failure.

4.1.5. Data-driven machine-learning-based seismic failure mode identification of reinforced concrete shear walls [9]

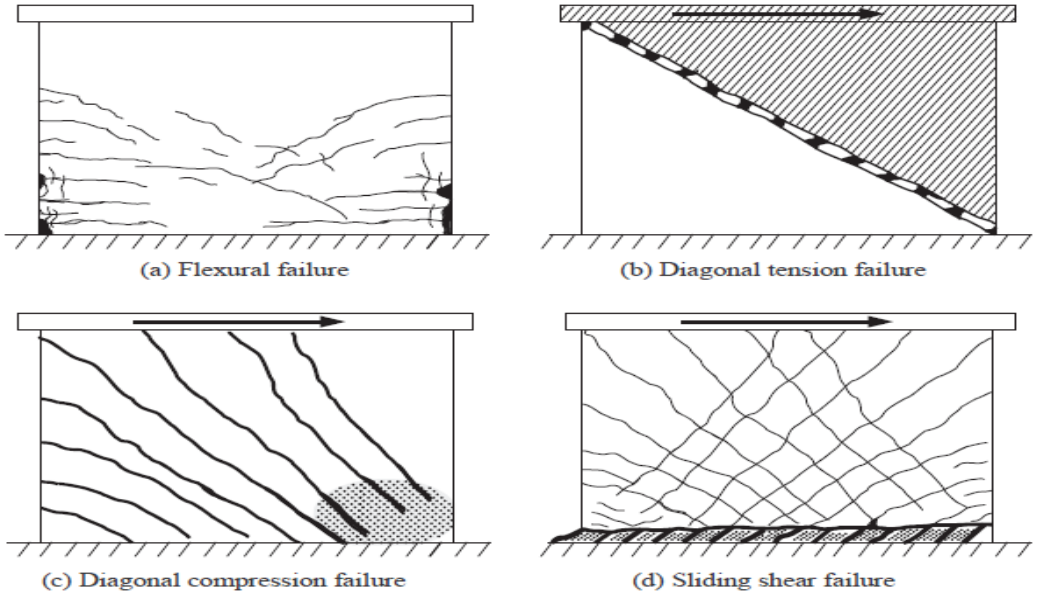

Figure (B) Various Shear Failure Mode of Shear Walls

Figure above shows four different shear failure mode of shear walls. Starting from figure a, due to fracture of longitudinal reinforcement or crushing of concrete causes wall to fail in flexure. Secondly, due to inadequate horizontal shear reinforcement "categorized by one or more corner-to-corner diagonal cracks", diagonal tension failure becomes unavoidable. Thirdly, for walls with proper horizontal shear reinforcement, it experiences concrete crush under diagonal compression with widespread crack patterns, hence causing diagonal compression failure. Finally sliding shear failure is a result of either

- Over a narrow band along wall base, rebars buckle and the crushing of concrete, as shown.
- Large cracks visible at wall base

In short, sliding shear is the shear failure of the wall when seismic load is applied along exact horizontal plane, while diagonal shear failure is shearing failure when load is applied at an angle to the horizontal plane.

Although the research paper devised ML program to predict failure mode identification with 84% accuracy, there isn't any exact empirical or ML approach to predict failure mode types. However, the paper indicates that the essential characteristics that determine failure modes include aspect ratio, boundary element reinforcement indices, and wall length-to-wall thickness ratio.

4.2. Size Effect of Squat Shear Walls Extrapolated by Micro plane Model [14]

The failure load of a squat wall is influenced by numerous factors: compressive strength of concrete, the boundary reinforcement ratio, the aspect ratio, cross section of the wall, transverse and vertical web reinforcement ratios and vertical axial force. Such factors lead to diverse failure mechanisms like diagonal tension, sliding shear and diagonal compression as shown above.
For shear walls with smaller aspect ratios, failure shifts from flexural to shear thanks to lesser cross-sectional area of the wall. Resultingly, size effect becomes of key importance for aspect ratios lesser than two. Concrete being a quasi-brittle material rather than plastic, size effect must be considered in further analysis.

From the research paper, following conclusions can be extracted for doubly reinforced S4 and singly reinforced S9 Shear walls of various sizes:

Table 3—Dominant failure mechanism for wall S4

	Half	Normal	Double	Quadruple
Low reinforced	Flexural	Flexural	Flexural	Flexural
Normally reinforced	Flexural	Flexural	Flexural	Sliding shear
Highly reinforced	Sliding shear	Sliding shear	Sliding shear	Sliding shear
Elongated wall	Flexural	Flexural	Flexural	Flexural

Table 4—Dominant failure mechanism for wall S9

	Half	Normal	Double	Quadruple
Low reinforced	Flexural	Flexural	Flexural	Flexural
Normally reinforced	Flexural	Diagonal tension	Diagonal tension	Diagonal tension
Highly reinforced	Diagonal tension	Diagonal tension	Diagonal tension	Diagonal tension
Elongated wall	Diagonal tension	Diagonal tension	Diagonal tension	Diagonal tension

Key points

- Smaller the aspect ratio, higher the chances of shear failure in concrete strut which in turn results in catastrophic brittle failure of the shear wall, which negates one of the intentions of having shear wall at first place- to have flexure-controlled failure to get inhabitants enough time to evacuate.
- Shear wall size doesn't play much role in slender shear walls in comparison to squat walls.
- Increasing steel ratio makes size effect to contribute to shear strength.
- Vertical steel bars prevent inclined shear cracks but remain in-active against sliding shear.
- Absence of horizontal bars may cause shear cracking and size effect.

4.2.1. Analytical model development

4.2.1.1. Mathematically

For D-region members, total shear strength is sum of the shear strength contributed by each of the force transfer mechanisms i.e, diagonal strut mechanism and truss mechanism as follows:

$$\mathbf{V_n = V_{nc} + V_w} \quad \text{……. (1)}$$

Where $\mathbf{V_{nc}}$ is the shear strength provided by diagonal strut mechanism and $\mathbf{V_w}$ represents truss mechanism's resulting shear strength, $\mathbf{V_n}$ is shear strength of the squat wall.

Moreover, Θs is strut inclined angle and is determined as follows:

$$\mathbf{\tan\Theta s = \frac{Hw}{Lw - hb}} \quad \textbf{(Θs should not be less than 25 as per ACI)}$$

Where h_w and l_w represent the height and length of the wall, respectively, and h_b represents the length of the boundary element. For uniformly distributed vertical bars in rectangular walls, boundary element length (h_b) is equal to $0.1L_w$, i.e, 10% of length the wall.

The following figure shows the simplified STM **(The dark line shows the diagonal strut, and the dotted lines show the ties).**

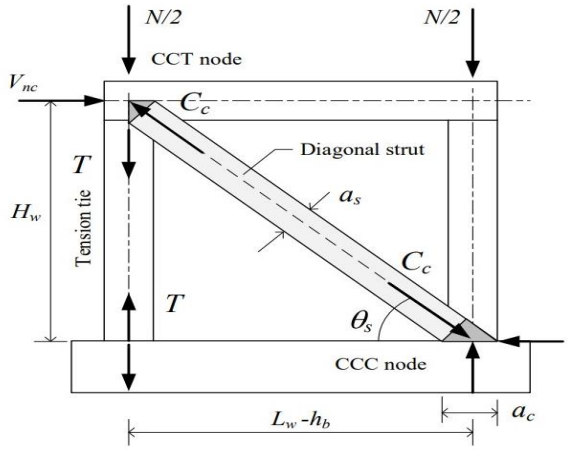

Figure (C) Simplified STM of squat wall

4.2.1.2. By using Diagonal Strut Mechanism

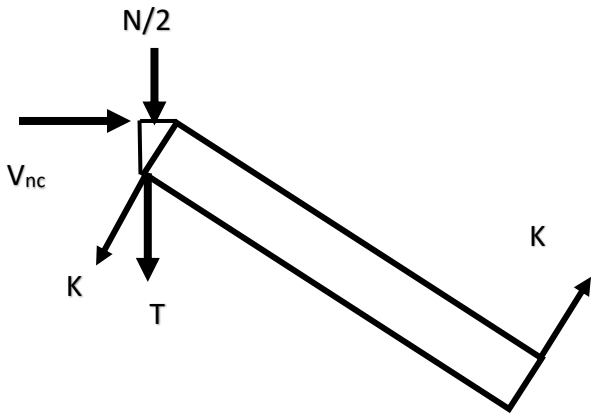

Fig (a)

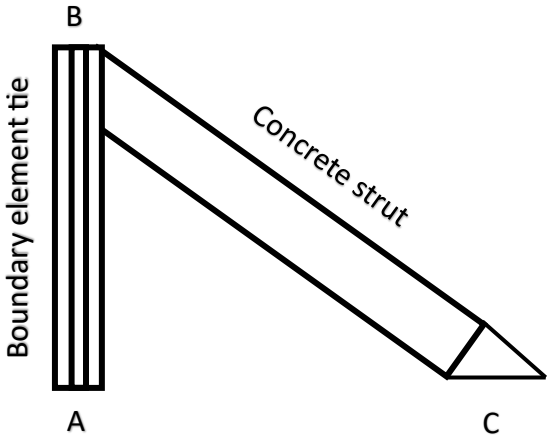

Fig (b)

We consider node C to obtain Mohr-column's criterion equation.

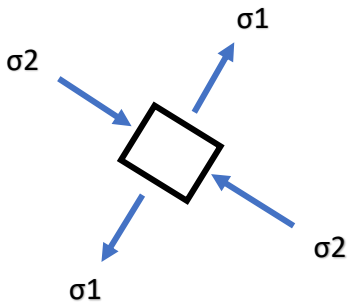

Fig (c)

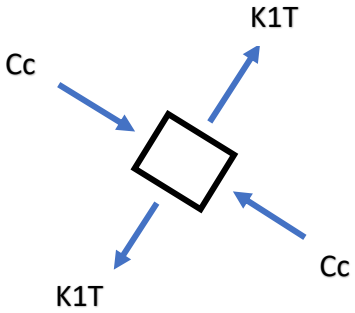

Fig (d)

Figure (c) shows concrete strut assumed biaxial state of stresses in at node C which is CCC node (which is bounded by three compressive forces). We resolve above figures using summation of forces along x and y axis as follows :

4.2.1.3. Principle tensile stress ($\alpha 1$)

$$\sigma 1 - k1T = 0$$

where T is the tension force which has been multiplied with K1- a force distribution factor to represent its distribution of tension throughout the diagonal strut. Hence,

$$\sigma 1 = k1T \text{.....(2)}$$

4.2.1.4. Principle compressive stress ($\alpha 2$)

$$\sigma 2 - Cc = 0$$

Here Cc is the compressive force generated inside the strut due to application of lateral force V_{nc} which in turn forces the assumed compressive strut to bulge out. Hence,

$$\sigma 2 = Cc \text{ .....(3)}$$

4.2.1.5. K1 stress distribution factor

Tang and Tan considered uniform/ rectangular stress distribution which is inaccurate in comparison to triangular stress distribution which causes both positive and negative stress distribution as shown.

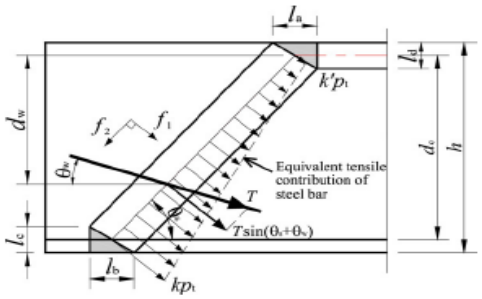

Fig. 1. Determination of tensile stress factors at nodal zones.

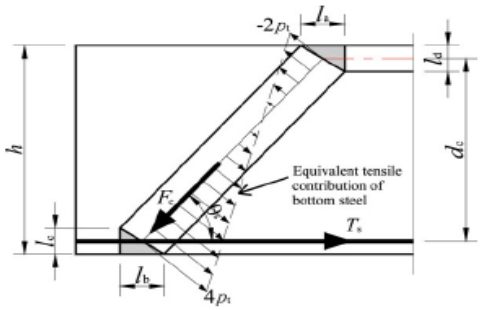

Fig. 2. Assumed tensile stress distribution arising from bottom steel.

Figure (D) Tensile Stress Distribution

Along the diagonal strut, triangular stress distribution can be assumed to cater for nonlinear changes in stress distribution as we can observe extra confinement at the bottom, in comparison to the top, and due to the presence of the bottom steel. Tan et al.[15] proposed k = 2, k being stress distribution constant, utilizing force equilibrium, by equating the force represented by the triangular stress block to Ts sin$\boldsymbol{\Theta s}$. We do know that though force equilibrium was satisfied at first place, violation of moment equilibrium was observed.

In order to satisfy both force and moment equilibrium, the stress distribution is shown in Fig. 2 and the constant for stress distribution, k, can be simultaneously calculated as follows. Although according to the paper, there is a minor 5% difference in strength when K is considered 2 instead of 1, yet this effect should be considered for appropriate results.

4.2.1.6. Applying Mohr- Coulomb failure criteria

For nodal zones (tension–compression stress state), Ning Zhang, Kang-Hai Tan model [16] utilizes a failure criterion using Mohr–Columb theory (Cook and Young 1985) from research paper [15] assumption of Tan et al, as below:

$$\frac{\sigma 1}{f_{tn}} + \frac{\sigma 2}{fc} = 1 \ldots\ldots (4)$$

Where σ2 =< fc keeping in view that bottom node is bounded in both directions(i.e, additional lateral confinement), ftn is the tensile strength provided by boundary reinforcement and concrete in σ1 direction and fcr is compressive strength of concrete cylinder, in σ2 direction.

Resolving Cc and T:

From The Given Tringle ABC as shown in previous figure (b)

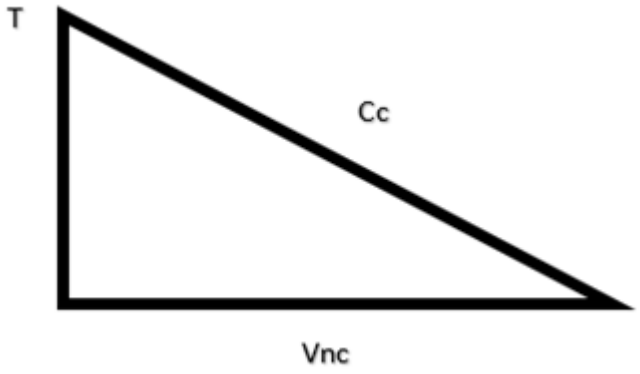

$$Cc = \frac{V_{nc}}{Cos\theta_s} \quad \ldots..(5)$$

$$T = V_{nc} tan\theta_s \ldots\ldots. (6)$$

N was expected to be quietly sensitive to T since most low-rise shear walls are subjected to relatively low axial load ratios (lower the height, lesser the earthquake loads)

V_{nc} is a factor which transforms the compressive force N into equivalent lateral force.

Softening coefficient:

Tan et al [15] suggests:

$$v = \frac{f_2}{f'_c} = 1 - \frac{f_1}{f_t} \leq 1$$

It is assumed that the strut has uniform cross-section along its length and is prismatic.

As we know, $stress = \frac{force}{Area}$

$$\boldsymbol{\alpha 2} = \frac{\boldsymbol{Cc}}{\boldsymbol{A_{str}}} \quad \text{……. (7)}$$

$$\boldsymbol{\&} \qquad \boldsymbol{\alpha 1} = \frac{\boldsymbol{k1T}}{\boldsymbol{As}} \quad \text{…….. (8)}$$

Here As is area of steel of any single boundary element upon which V_{nc} is to be assumed against which shear strength is being determined. Furthermore, A_{str} is the cross-section area of the strut, and it can be represented by the product of wall web and depth of diagonal strut.

$$\boldsymbol{A_{str} = t_w * as}$$

Here, **as** is the depth of diagonal strut and $\mathbf{t_w}$ is thickness of wall web.

For the depth of the flexural compression zone of an elastic column, Hwang [17], using Paulay and Priestley's (1992) equation, suggested that as is approximately equal to depth of flexure compression zone ac. (*"Eq 4.61, P273-74 of Seismic Design of Reinforced Concrete and Masonry Buildings"* by T. Paulay)

$$ac = as = \left(0.25 + 0.85\frac{N}{A_w f c}\right) l_w$$

Here A_w= concrete section net area bounded by l_w and t_w, namely shear force directional length of the wall and web thickness, respectively, and $\frac{\boldsymbol{N}}{\boldsymbol{A_w f'c}}$ is the axial load ratio, N being minimum compression force

Using equations 5 and 6 in 7 and 8:

$$\alpha 2 = \frac{V_n}{A_{str} Cos\Theta s}$$

$$\& \quad \alpha 1 = \frac{k1 V n tan\Theta s}{As}$$

Substituting Values in equation 4 we get:

$$V_{nc} = \frac{1}{\frac{k1 tan\Theta s}{As\, f_{tn}} + \frac{1}{A_{str} Cos\Theta sfc}} \quad \ldots\ldots\ldots \text{(a)}$$

4.2.1.7. By using Truss Mechanism

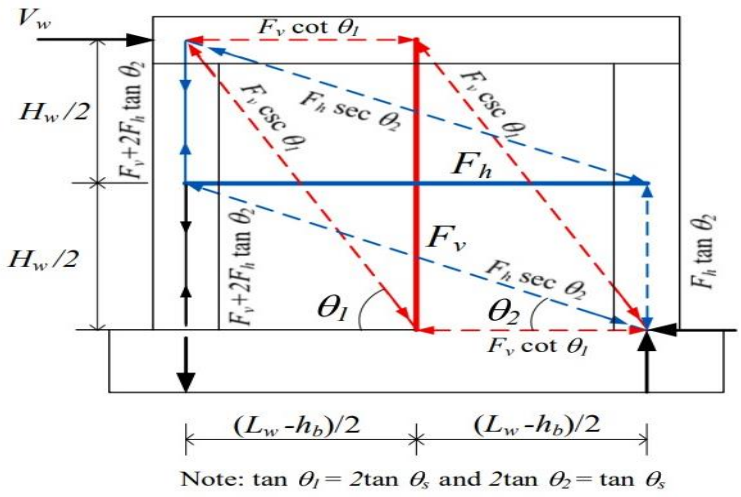

Figure (E) Truss Mechanism

The truss mechanism constitutes sub trusses in vertical and horizontal directions. The shear strength contributed by these sub trusses is mainly governed by the two ties (vertical and horizontal).

By providing an additional loading path for transfer of squat wall lateral forces, the presence of web reinforcements may activate greater shear resistance in addition to diagonal system. The horizontal truss mechanism consists of one lumped (assumed) horizontal tie (blue solid line), two

vertical members and two flat struts represented by dashed lines in blue. Moreover, the vertical truss mechanism consists of one lumped (assumed) vertical tie (red solid line), two horizontal members and two steep struts represented by dashed lines in red.

By force equilibrium, Fx = 0;

$$\boldsymbol{V_w = F_h + 2F_v cot\Theta 1}$$

$$\boldsymbol{V_w = F_h + \left(\frac{2F_v}{tan\Theta 1}\right)}$$

$$\boldsymbol{V_w = F_h + \left(\frac{2F_v}{2tan\Theta s}\right)}$$

$$\boldsymbol{V_w = F_h + F_v cot\Theta s}$$

Squat shear walls generally fail in shear therefore the horizontal and vertical reinforcement may not attain their yield strength. Changing the equation to:

$$\boldsymbol{V_w = K_h A_h F_{yt} + K_v A_v f_{yv} Cot\Theta s}\text{.....(b)}$$

Using equation (a) and (b) in equation 1:

$$V_n = \frac{\mathbf{1}}{\frac{\boldsymbol{k1tan\Theta s}}{\boldsymbol{Asf_{tn}}} + \frac{\mathbf{1}}{\boldsymbol{A_{str}Cos\Theta sfc}}} + \boldsymbol{K_h A_h F_{yt} + K_v A_v f_{yv} Cot\Theta s}$$

Here:

- K1 (Transverse stress distribution factor)
- $\boldsymbol{\Theta s}$ (Depends on Squat wall dimensions)
- A_{be} is equal to $\rho_{be}(b_b x h_b)$
- A_h is equal to $\rho_h(H_w x t_w)$
- A_v is equal to $\rho_v(L_w - h_b)t_w$
- Where $k_h = 0.11$ and $kv = 0.19$ from Gulec and Whittaker and Ma et al.[19]
- For K1, from (N. Zhang, K. H. Tan)

Comparing Eqs. (6) and (7), for top and bottom nodal zones, the principal tensile stress can

be determined using following factors:

$k` = 4 - 6 \cdot (d_w / d_c)$

$k = 6 \cdot d_w / d_c - 2.$

- f_{tn} is concrete's tensile strength and boundary vertical reinforcement, Tang, and Tan et al [18] suggests:

  That the tensile strength of longitudinal reinforcement and concrete in the boundary elements:

$$Asf_{\text{tn}} = A_{be}f_{ybe} + 0.5\sqrt{fc}\, b_b\, h_b$$

- Where fc is the compressive strength of concrete.
- f_{ybe} is boundary element yielding strength.
- b_b is boundary element thickness and h_b is boundary element width and Abe is boundary element steel area.

  In other words, Asf_{tn} accounts for concrete and boundary element steel tensile strength.
- For w = 0 and $d_w = d_c$ (bottom reinforcement (Fig. 2)), the stress distribution factor is:

  $k` = -2$ (compression)

  k = 4 (tension). Hence for tensile forces due to bottom reinforcement, take k1=4.

4.2.2. Determination of optimum parameters for proposed model

The optimum values of K_h and K_v were found to be equal to 0.11 and 0.19 respectively by performing non-linear regression using FIMCON function of MATLAB. Gulec and Whittaker[19] and Ma et al can be referred to for detailed understanding the parameters optimization. “Strut and Tie model for predicting shear strength of squat walls under earthquake loads” paper by Panatchai Chetchotisak[10] can be referred to as for the determination of values of the parameters as this procedure was out scope of our Final Year Project.

FIMCON function can be illustrated as follows:

$$A_x =< b$$

$$A_{eq}x = b_{eq}$$

$$min_{\ x}\ f(x) \text{ subject to } C(x) =< 0$$

$$C_{eq}(x) =< 0$$

$$Lb =< x =< ub$$

Here $f(x)$ represents the design variable's x, objective function i.e, a, k_h *and* k_v; b and b_{eq} being the vector coefficients of corresponding matrices, A and A_{eq} are coefficient matrices of linear equality and inequality constraints, respectively.

Of the variables *x, ub and lb* are vectors of upper and lower bounds, respectively. C(x) and C_{eq} (x) are nonlinear functions of equality and inequality constraints.

5. MODEL DESIGN

A sample, step by step design calculations can be shown as follows:

Given Data:

H_w = Height of wall	;	h_b = Height of boundary element
L_w = Length of wall	;	b_b = Width of boundary element
f_c = Compressive strength	;	t_w = Web thickness
fy_h = Yield Strength of H.bars	;	fy_v = Yield strength of V.bars
ρ_h = Reinforcement ratio of H.bars	;	ρ_v = Reinforcement ratio of H.bars

Step#1:

$$\mathbf{tan\Theta s = \frac{Hw}{Lw - hb}}$$

Step#2:

$$\boldsymbol{ac = as = \left(0.25 + 0.85\frac{N}{Awfc}\right) lw}$$

Step#3:

$$A_{str} = t_w * as$$

Step#4:

$$Asf_{tn} = A_{be}f_{ybe} + 0.5\sqrt{fc}\, b_b\, h_b$$

Step#5:

$$A_h = \rho_h\, H_w\, t_w$$

Step#6:

$$A_v = \rho_v\, L_w\, t_w$$

Step#7:

$$V_{nc} = \frac{1}{\frac{k1tan\Theta s}{A_s f_{tn}} + \frac{1}{A_{str} Cos\Theta sfc}}$$

Step#8:

$$V_w = K_h A_h F_{yt} + K_v A_v f_{yv} Cot\Theta s$$

Step#9:

$$V_n = V_{nc} + V_w$$

6. VALIDATION

6.1. Validation through Abaqus

Abaqus CAE software was used to find the shear strength and deflections of the proposed model. The dimensions and materials specifications were taken from literature (Size Effect of Squat Shear Walls Extrapolated by Microplane Model M7 by Mohammad Rasoolinejad and Zdeneˇ k P. Bažant) in order to validate Abaqus model first and subsequently the analytical model. The figure below shows the dimensions and reinforcement details.

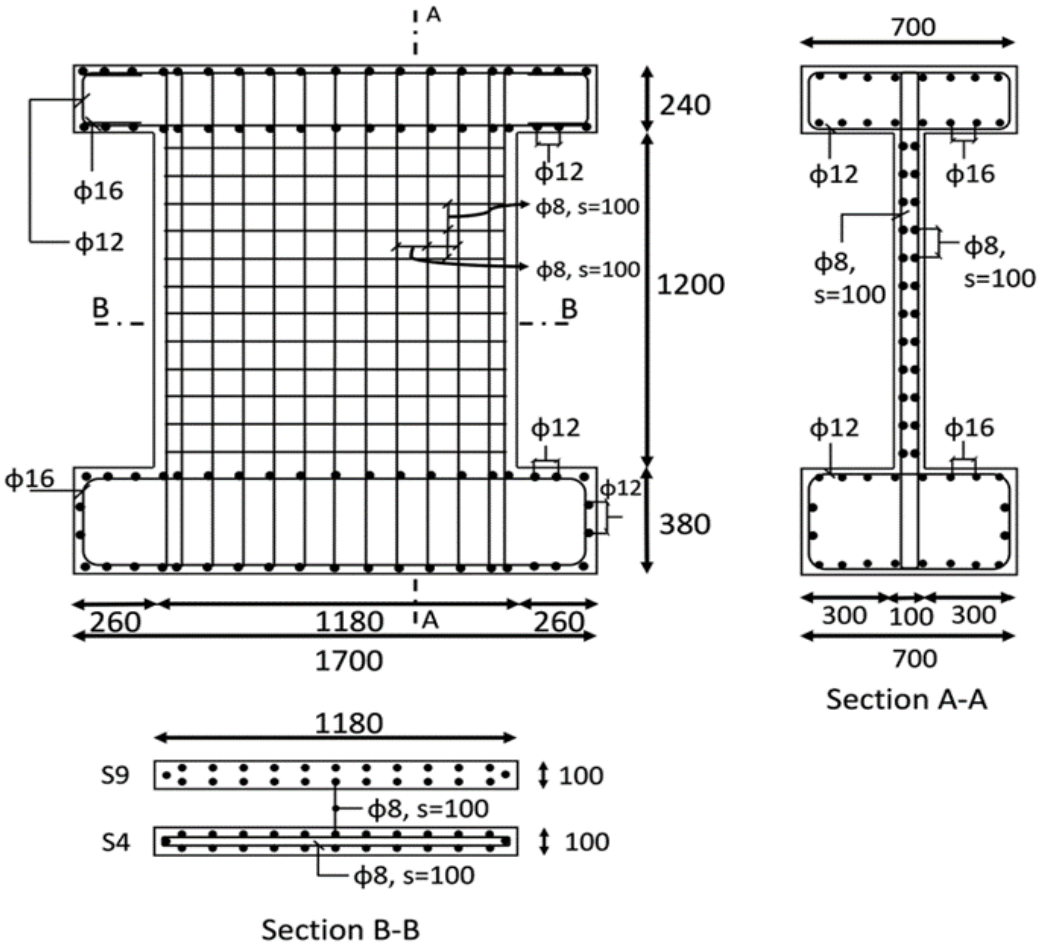

Figure (F) Various cross sections shows the reinforcement details of squat shear wall

For the materials normal concrete with compressive strength of 30 Mpa was used, and the reinforcement used had a yield strength of 574 Mpa. All the parts of the model were made separately and then assembled as shown.

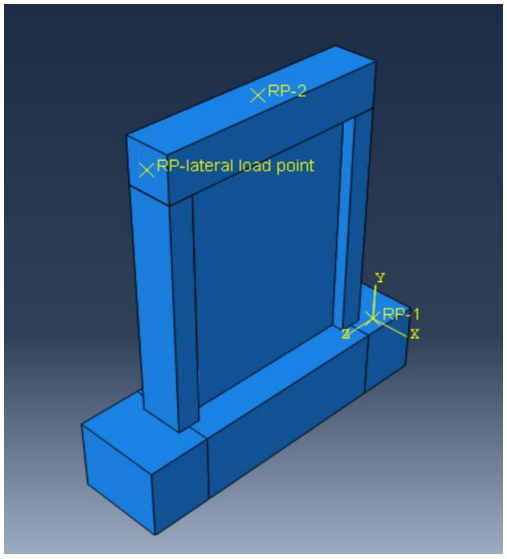

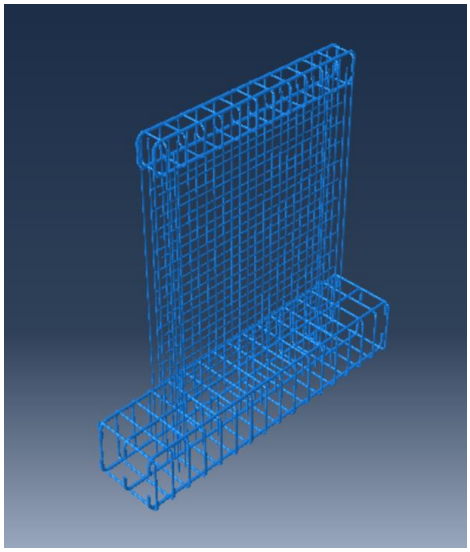

After making the parts and assembling them the model was meshed with concrete parts having mesh size of 50mm and reinforcement with 20mm size. The mesh type used for concrete parts was C3D8I and for rebars it was T3D2. The figure below shows meshing done through the web and whole wall.

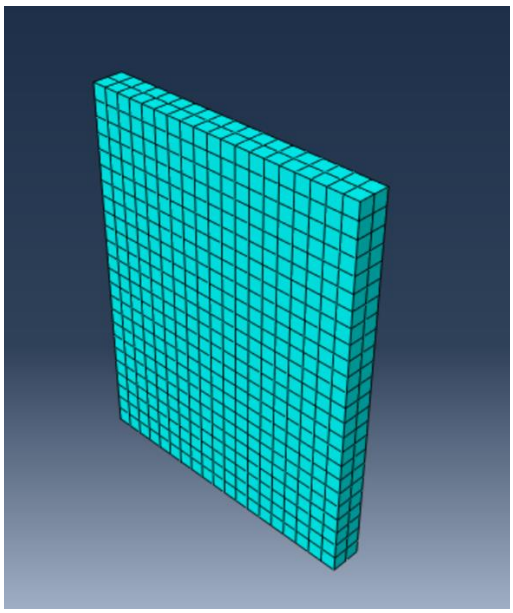

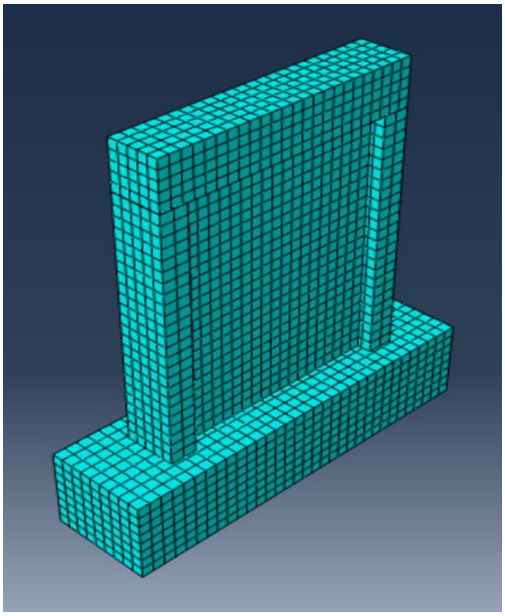

After meshing the parts, the loads were applied and the analysis were run and the results can be seen in the visualization module. The figures below show the stresses developed in concrete and later displacement of the wall.

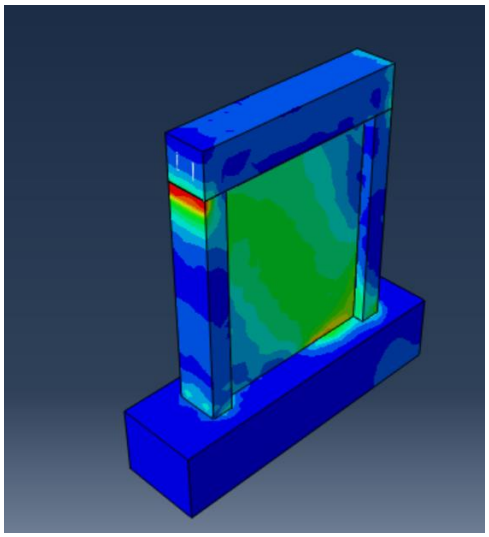

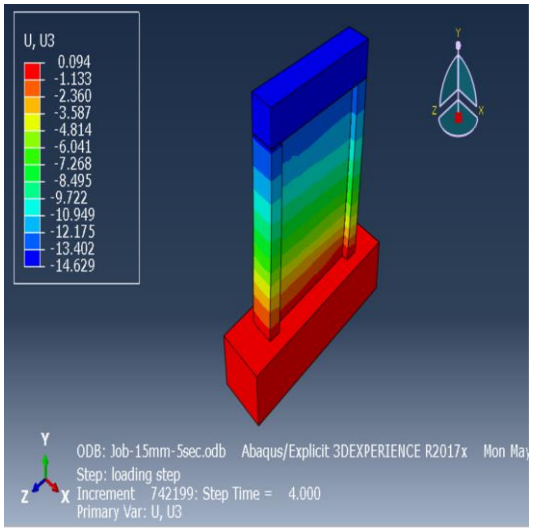

In order to check whether our finite element model is giving correct results we compared the displacement at maximum load of our model with the research paper from where we have taken the dimensions and materials specifications and the results are shown below.

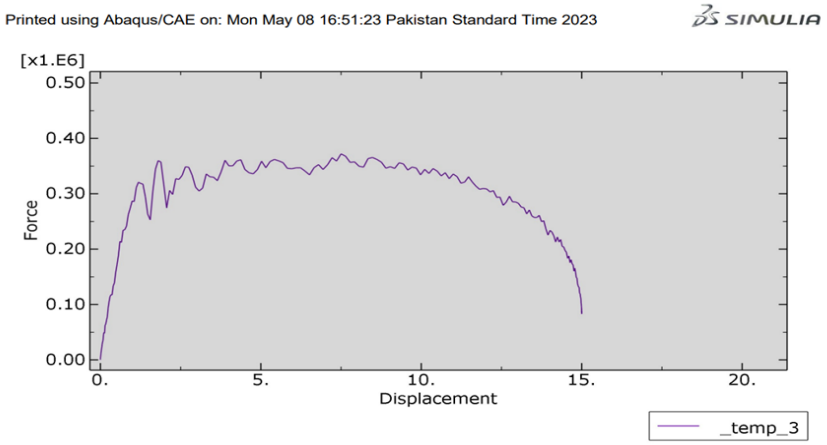

Figure (G) Force-Displacement Graph obtained from Abaqus Model

Wall	Geometry	ρ_x, 10^{-2}	ρ_y, 10^{-2}	F_v, kN (kip)	F_h	Maximum load, kN (kip)	Displacement at maximum load, mm (in.)
S4	Rectangular	1.03	1.05	–262 (–58.9)	Monotonic	392 (88.1)	11.44 (0.45)
S9	Rectangular	0.0	9.9	–260 (–58.4)	Monotonic	342 (76.9)	9.09 (0.36)

Figure (H) Results from research paper in the form of max load, force, and displacement

The outcomes obtained from our model are depicted in Figure (G) while the results from the research paper are depicted in Figure (H). The maximum load recorded for our model was 372 kN, while the lateral displacement was 8.06mm. These values are well in the range of the values given in the mentioned paper which proves the validity of our Abaqus model. Further the same dimensions and material specifications were put in the developed analytical model and the strength coming from that was 388 kN. The ratio of the analytical strength and finite element model strength was then compared to the ratios in the literature to further validate the developed model. The results are shown below.

Comparison of experimental (Vpeak) peak shear strengths to those predicted (Vpeak FE) for squat walls

Program ID	Wall ID	V_{peak} (kN)	V_{peak_FE} (kN)	V_{peak_FE}/V_{peak}
Chiba	1	1658	1496	0.9
	3	1475	1506	1.02
	4	1677	1663	0.99
	5	1823	1819	1
	6	1515	1603	1.06
	7	1617	1812	1.12
	8	1343	1260	0.94
Yagishita	2	1246	1298	1.04
	3	1307	1345	1.03
	6	1146	1177	1.03
Fukuzawa	1	1192	1041	0.87
	2	1283	1278	1
	3	2003	1834	0.92
	4	1732	1823	1.05
	5	744	635	0.85
	6	1421	1139	0.8
	7	1151	975	0.85
	8	1698	1602	0.94
	9	1871	1709	0.91
	10	1275	1123	0.88
	11	2081	2150	1.03
	12	1656	1584	0.96
PROPOSED MODEL	1	388	372	0.96

6.2. Validation through experimental data

The data of 126 walls (attached with **Appendix-A**) from the literature was entered in the proposed model and the shear strength was obtained, further the same data was put in the other 8 state of the art models and their respective shear strengths were calculated and the compared with the proposed model. Excel file was developed to derive shear strength of squat wall database values available online, and resulting shear strength were compared with experimental values. Co-efficient of determination (R^2) were obtained. Finally respective Co-efficient of determination (R^2) were compared with our model. Our model had an (R^2) of 0.9604. Hence it proves that our model performs well for rectangular squat shear walls of respective databases. The following shows content from the excel file.

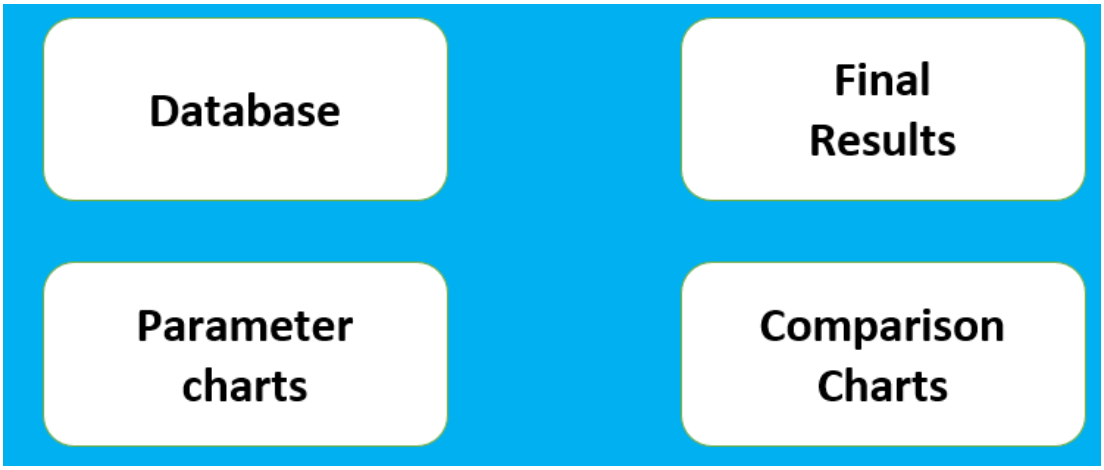

Frequency charts:

Figure (I) shows the frequency of different parameters of the experimental database.

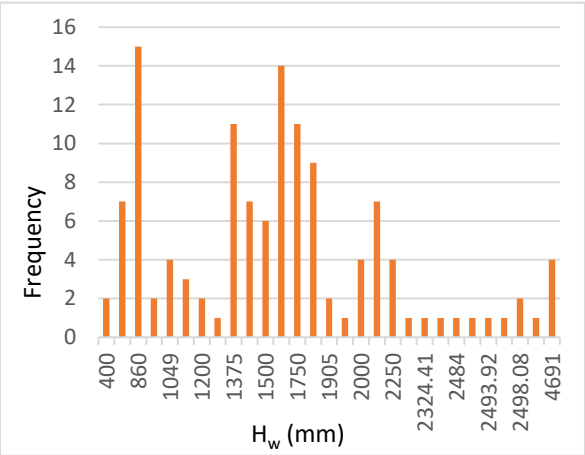

a) Frequency vs Height of Wall

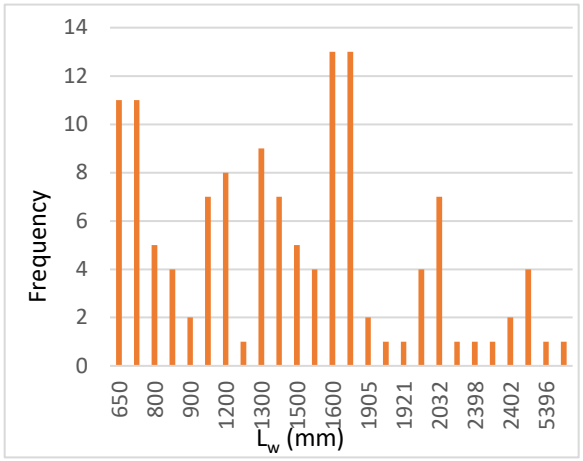

b) Frequency vs Length of Wall

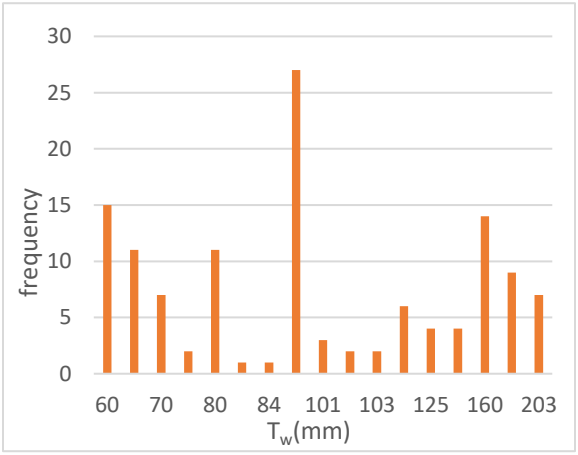

d) Frequency vs Thickness of Wall

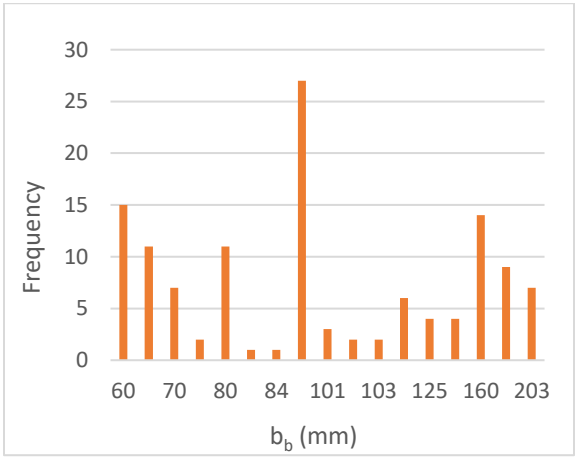

c) Frequency vs Width of Boundary Element

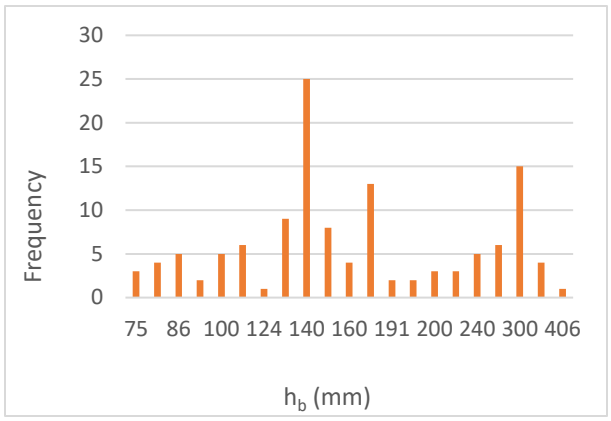

e) Frequency vs Height of Boundary Element

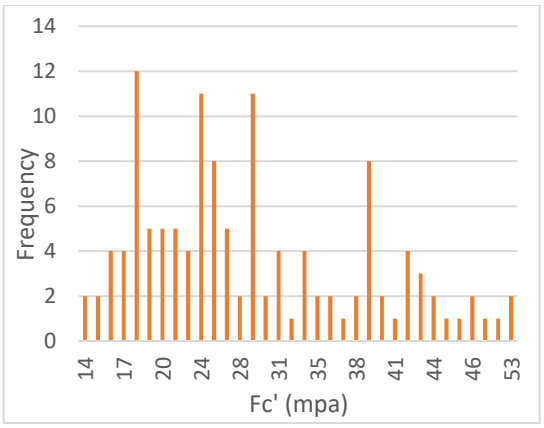

e) Frequency vs Compressive Strength

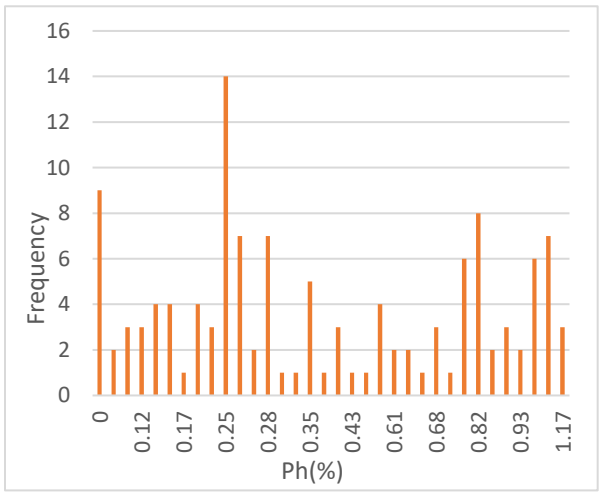

g) Frequency vs Horizontal Reinforcement Ratio

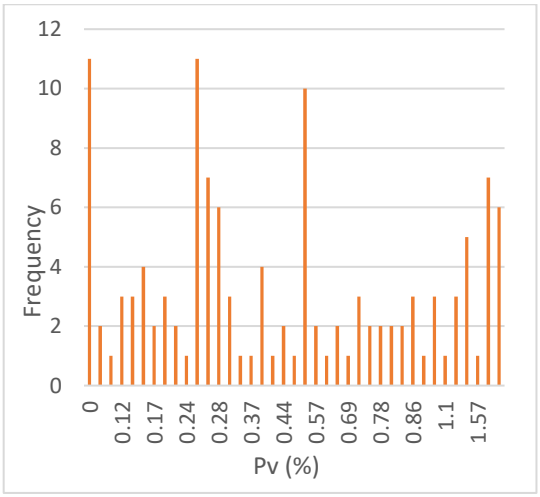

h) Frequency vs Vertical Reinforcement Ratio

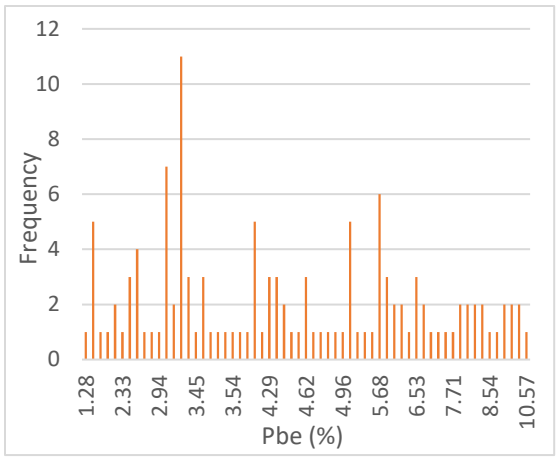

i) Frequency vs Boundary Element Reinforcement Ratio

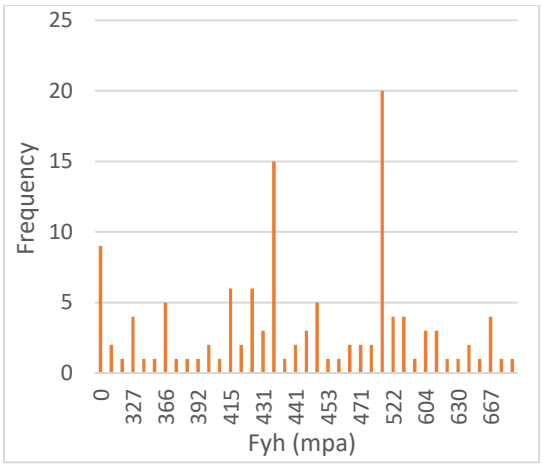

j) Frequency vs Vertical Reinforcement Yield Strength

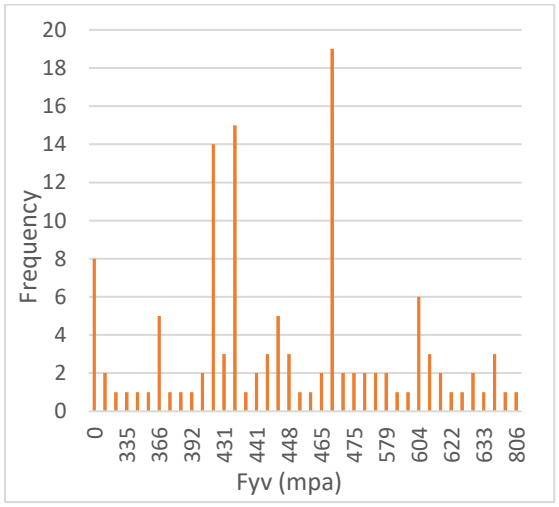

k) Frequency vs Vertical Reinforcement Yield strength

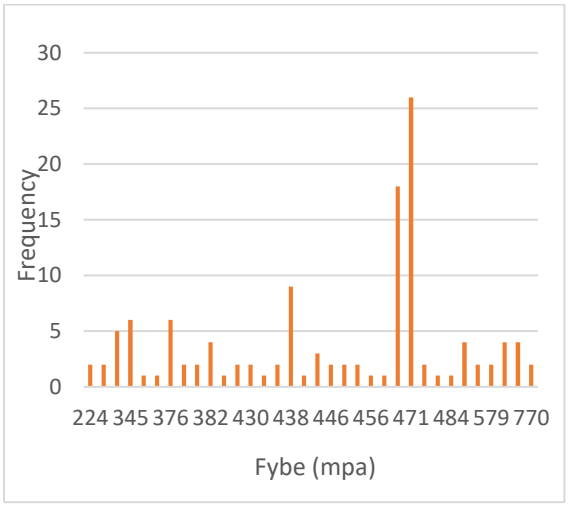

l) Frequency vs Boundary Element Yield Strength

Figure (I) Frequency vs various parameters of Squat Shear Wall

Parameters charts:

Figure (J-a) presents the model accuracy of the wall height (Hw) with a value of 1.00 indicating the satisfactory performance of the proposed model across various levels of Hw ranging from 0.5 to 1.5. Likewise, other figures illustrates the accuracy of other influential parameters such as Lw, Tw, Fyh, Fyv, Pv, and P, all of which exhibit an acceptable accuracy value of 1.00. Therefore, based on the analysis of the experimental data, it can be confirmed that the proposed model demonstrates a reliable predictive capability.

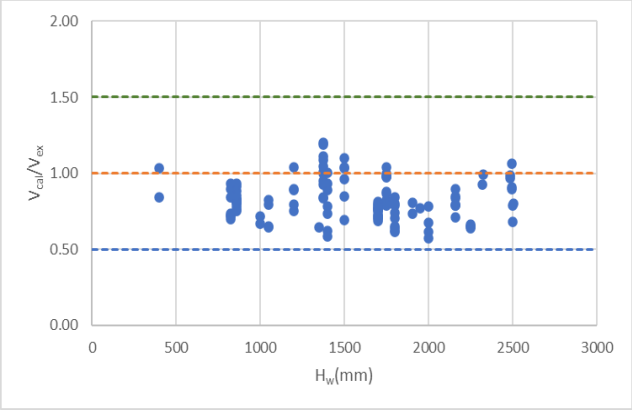

a) Shear Strength ratio vs Height of Wall

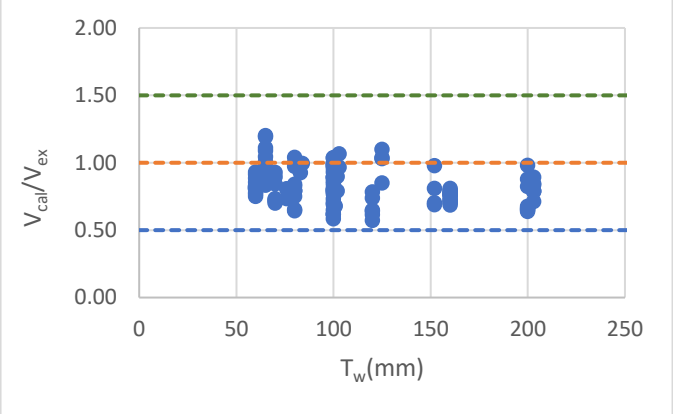

b) Shear Strength ratio vs wall thickness

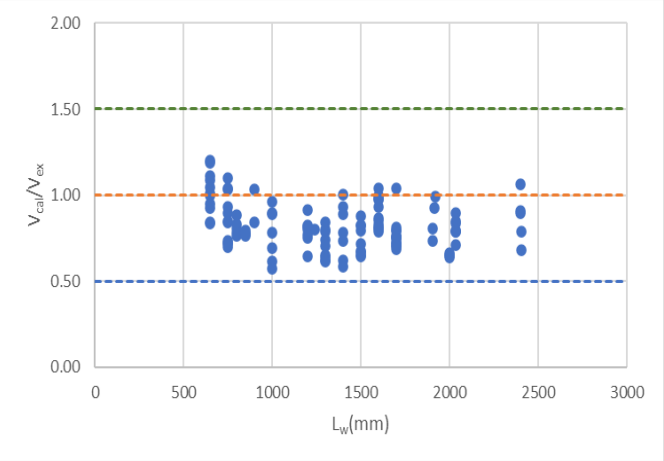

c) Shear Strength Ratio vs Length of Wall

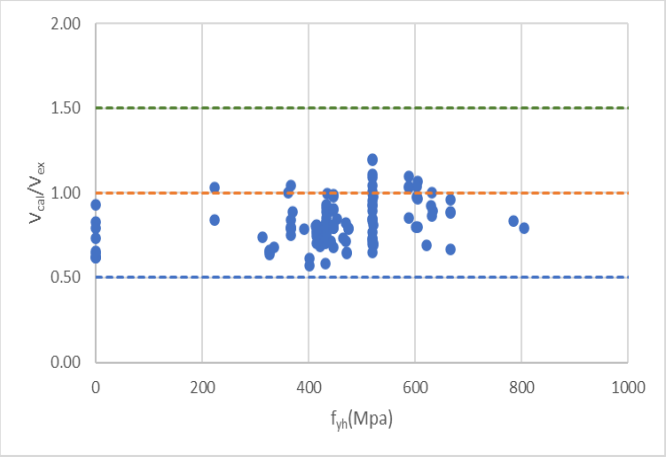

d) Shear Strength ratio vs Horizontal Reinforcement Ratio

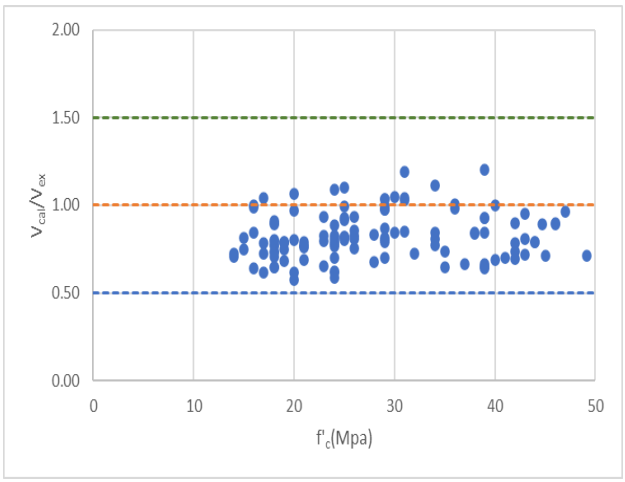

e) Shear Strength Ratio vs Compressive Strength

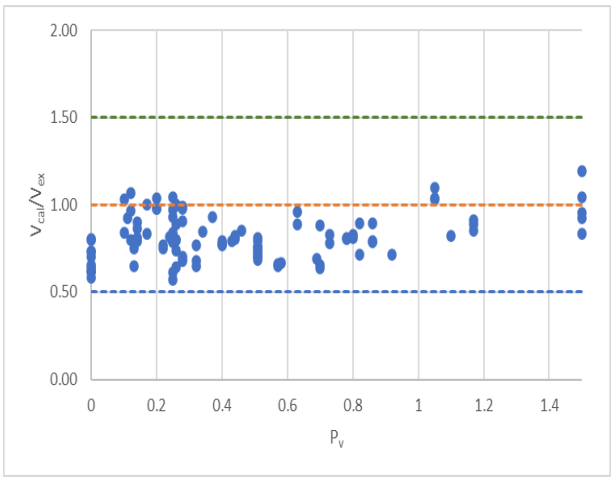

f) Shear Strength Ratio vs Vertical Reinforcement Ratio

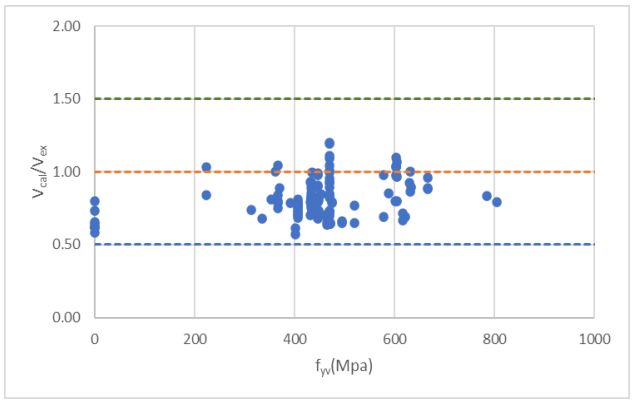

g) Shear Strength ratio vs Vertical Reinforcement Yield Strength

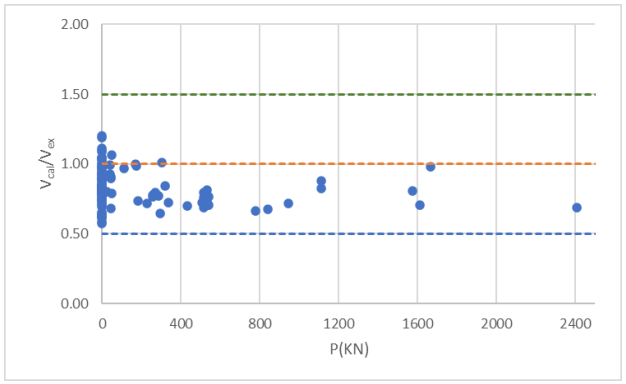

h) Shear Strength ratio vs Axial Load

Figure (J) Graphs of the Shear Strength ratio of calculated over experiment vs various parameters of Squat Shear Wall

7. RESULTS

The effectiveness of an empirical model depends on how the model is trained and validated using the provided dataset. To create the model, 126 of the designated walls with boundary element were selected as training data, shear strengths obtained from various models including proposed model of 126 walls are attached with **Appendix-B**. Various statistical methods can be used to analyze and gain numerical understanding of the proposed STM model.

The coefficient of determination (R^2) is one of the most popular statistical approaches to testing model reliability. The coefficient of determination equal to one is considered to provide the best fit.

$$R^2 = 1 - \frac{\sum[V_{jh}^{Exp} - V_{jh}^{Est}]^2}{\sum[V_{jh}^{Exp} - V_{jh(mean)}^{Est}]^2}$$

It is worth noting that the value of R^2 of the proposed model was 0.9604 which is superior to all the existing model for squat shear walls.

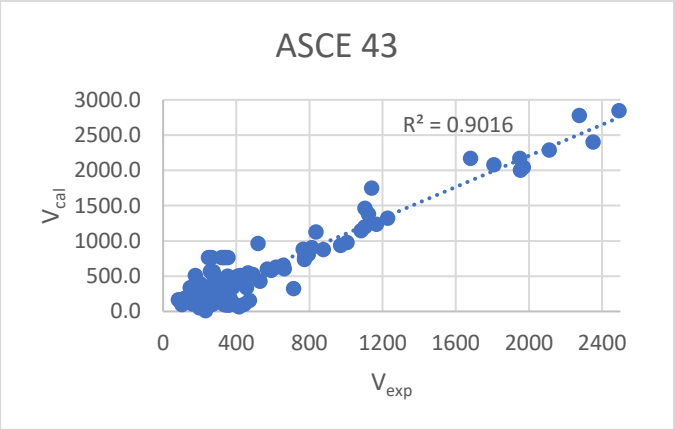

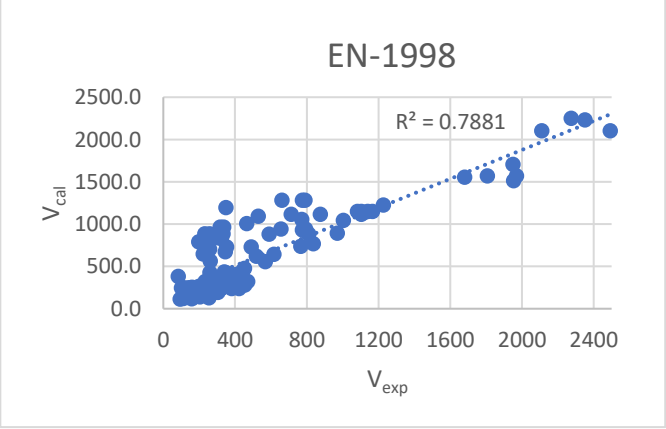

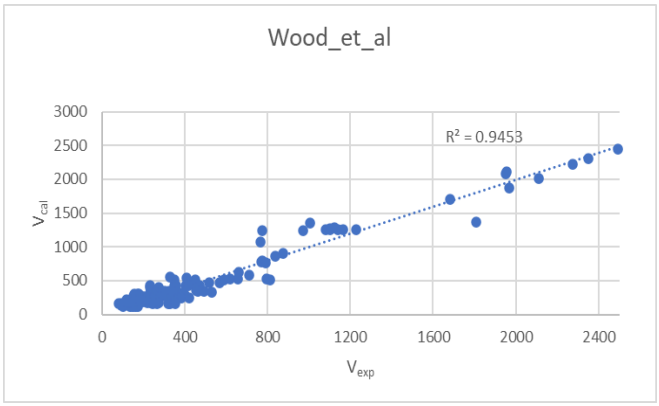
Wood_et_al
R² = 0.9453
V_cal
V_exp
0
500
1000
1500
2000
2500
3000
0
400
800
1200
1600
2000
2400

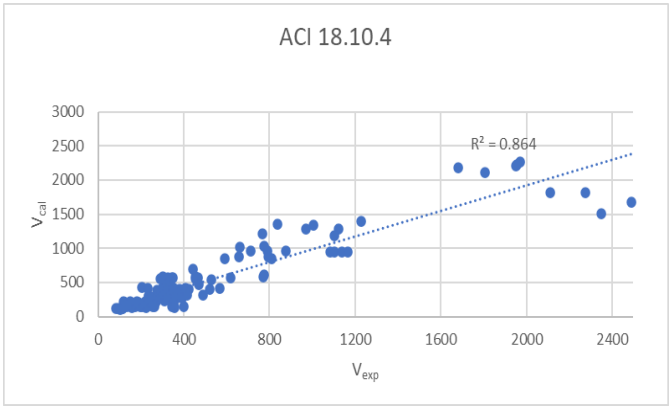
ACI 18.10.4
R² = 0.864
V_cal
V_exp
0
500
1000
1500
2000
2500
3000
0
400
800
1200
1600
2000
2400

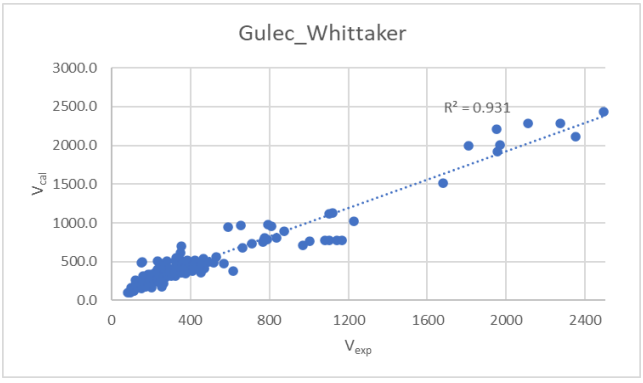
Gulec_Whittaker
R² = 0.931
V_cal
V_exp
0.0
500.0
1000.0
1500.0
2000.0
2500.0
3000.0
0
400
800
1200
1600
2000
2400

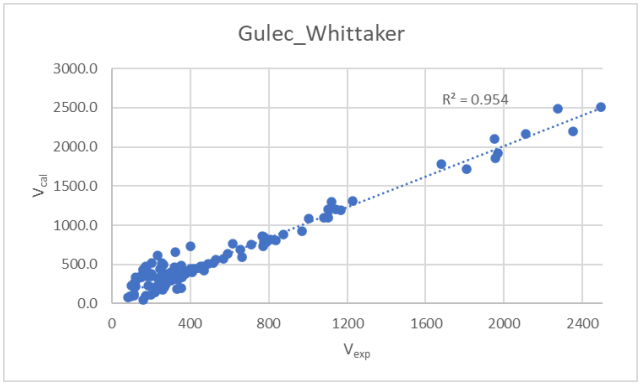
Gulec_Whittaker
R² = 0.954
V_cal
V_exp
0.0
500.0
1000.0
1500.0
2000.0
2500.0
3000.0
0
400
800
1200
1600
2000
2400

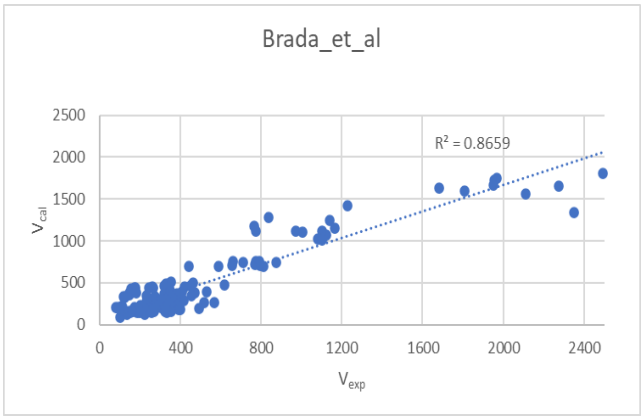

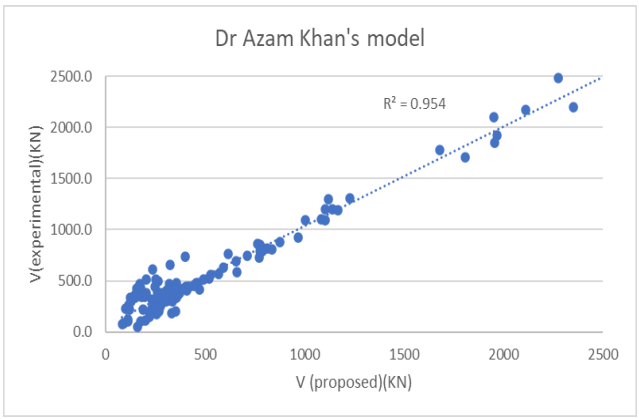

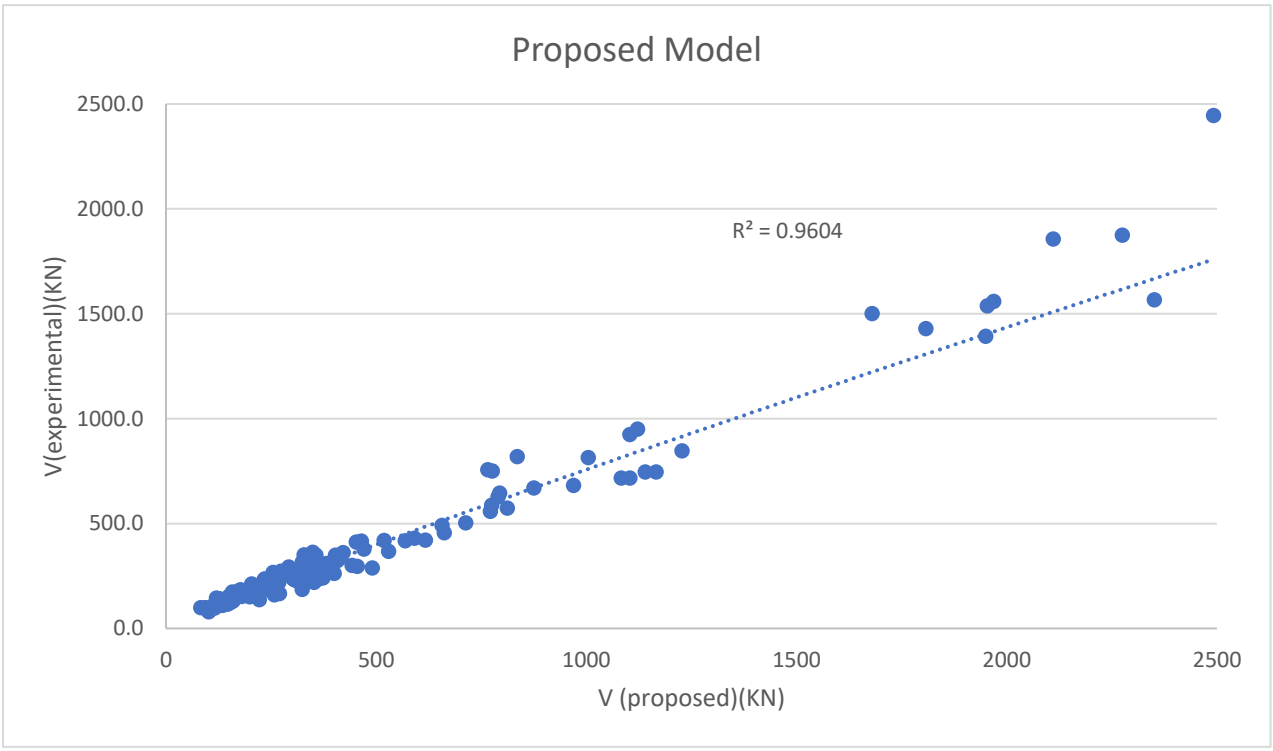

Figure (K) Graphs and comparison of the Coefficient of Determination of various models and proposed model of Squat Shear Wall

8. CONCLUSION

This research study focuses on the development of an analytical model using the Strut and tie (STM) approach to predict the shear strength of squat walls with boundary elements. The experimental data set consists of 126 walls, which were utilized to evaluate the shear strength predictions made by the proposed analytical model. In order to assess the model's performance, the same database was employed in eight other state-of-the-art models, and a comparison was made using the coefficient of determination (R^2) approach. The results demonstrated that the proposed model achieved an R^2 value of 0.9604, surpassing all existing models for squat shear walls. Additionally, an Abaqus model was constructed, allowing for a comparison of shear strength ratios between the analytical model and the Abaqus model. The obtained ratio was determined to be 0.96, which was subsequently compared with ratios reported in the literature, thereby providing further validation for the proposed analytical model.

9. LIMITATIONS / PROJECT EXTENSIONS

Our model has following limitations which can be overcome by extending scope of the project:

- Model gives good results for a set of 126 walls. Empirical equations can be extended to more data sets to account for study of variations in different squat walls parameters.

- The model was developed for rectangular squat shear walls only. For other types of shear walls like Barbell and flanged, modifications in the model can be made.

- K1, Kh and Kv parameters determined by MATLAB were referred to research papers available online. Non-linear regression can be performed on vast data sets available.

- More parameters can be introduced to account for assumptions mentioned at the start of the thesis document.

- Small scale experiments can be performed on squat shear walls by casting and curing for 28 days, to validate results obtained from the strut and tie model and ABAQUS with experimental values.

- Model scope can be further extended to flexure and diagonal flexure failure design of intermediate and slender shear walls specifying it as second part of the model for aspect ratios more than 2.

- Model results can further be compared with strut and tie models developed by other researchers except mentioned in the document.

10. REFERENCES

[1] Gupta, S. P. (2015). Building Construction. New Delhi*: PHI Learning Private Limited.*

[2] Massone, L. M., Orakcal, K., and Wallace, J.W. (2006). Modeling of squat shear walls controlled by shear.
Available at : https://www.iitk.ac.in/nicee/wcee/article/14_05-03-0025.PDF

[3] Gassone, L.M. and Wallace, J.W., 2004.Seismic response of reinforced concrete walls. ACI structural journal, 101(3), pp.304-312.

[4] J. K. Wight and J. G. MacGregor, Reinforced Concrete: Mechanics and Design, 7th ed., Pearson Education, 2019.

[5] Ismail, K.S., Guadagnini, M. orcid.org/0000-0003-2551-2187 and Pilakoutas, K. orcid.org/0000-0001-6672-7665 (2018) Strut-and-Tie Modeling of Reinforced Concrete Deep Beams. Journal of Structural Engineering, 144 (2). ISSN 0733-9445.
Available at : https://www.researchgate.net/publication/322221966_Strut-and-Tie_Modeling_of_Reinforced_Concrete_Deep_Beams

[6] Dr. Salah E. El-Metwally /et al/ Engineering Research Journal 155 (September 2017) C47 – C67
Available at : https://www.researchgate.net/publication/342377883_STRUT-AND-TIE_MODEL_VERSUS_NONLINEAR_FINITE_ELEMENT_ANALYSIS_OF_RC_CONTINUOUS_DEEP_BEAMS_WITH_AND_WITHOUT_OPENINGS#pf2

[7] Zhang, X., Liu, Y., Wang, Y., & Zheng, W. (2020). Convolutional neural network for damage classification of reinforced concrete shear walls subjected to seismic loads. Structural Control and Health Monitoring, 27(9), e2747.

[8] Guo, J., Li, J., & Wang, H. (2020). Seismic failure mode identification of reinforced concrete shear walls using a deep neural network. Structural Health Monitoring, 19(5), 1675-1690.

[9] Mangalathu, S., Jang, H., Hwang, S.-H., & Jeon, J.-S. (2020). Data-driven machine-learning-based seismic failure mode identification of reinforced concrete shear walls. Engineering Structures, 208, 110331.
Available at : https://doi.org/10.1016/j.engstruct.2020.110331

[10] Chetchotisak, P., Chomchaipol, W., Teerawong, J., & Shaingchin, S. (2022). Strut-and-tie model for predicting shear strength of squat walls under earthquake loads. Engineering Structures, 256, 114042.
Available at : https://doi.org/10.1016/j.engstruct.2022.114042

[11] Wael Kassem. (2015). Shear strength of squat walls: A strut-and-tie model and closed-form design formula.
Available at : https://doi.org/10.1016/j.engstruct.2014.11.027

[12] Direct strut-and-tie model for single span and continuous deep beams (by Ning Zhang, Kang-Hai Tan) - Engineering Structures 29 (2007) 2987–3001
Available at : http://dx.doi.org/10.1016/j.engstruct.2007.02.004

[13] Ma J, Ning CL, Li B. Peak shear strength of flanged reinforced concrete squat walls. J Struct Eng 2020;146(4):04020037.
Available at : https://doi.org/10.1061/(asce)st.1943-541x.0002575

[14] (Size Effect of Squat Shear Walls Extrapolated by Microplane Model M7) – by Mohammad Rasoolinejad and Zdeneˇ k P. Bažant.
Available at : http://www.civil.northwestern.edu/people/bazant/PDFs/Papers/603.pdf

[15] Tan KH, Tong K, Tang CY. Direct strut-and-tie model for prestressed deep beams. J Struct Eng 2001;127(9):1076–84.

[16] Direct strut-and-tie model for single span and continuous deep beams (by Ning Zhang, Kang-Hai Tan) - Engineering Structures 29 (2007) 2987–3001
Available at : http://dx.doi.org/10.1016/j.engstruct.2007.02.004

[17] Hwang SJ, Fang WH, Lee HJ, Yu HW. Analytical model for predicting shear strength of squat walls. J Struct Eng ASCE 2001;127(1):43–50.

[18] Interactive mechanical model for shear strength of deep beams. J Struct Eng 2004;130(10):1534–44. by Tang CY, Tan KH.
Available at : https://doi.org/10.1061/(ASCE)0733-9445(2004)130:10(1534)

[19] Gulec CK, Whittaker AS. Empirical equations for peak shear strength of low aspect ratio reinforced concrete walls. ACI Struct J 2011;108(1):80–9.

APPENDIX-A

No.	Ref.	Specimen ID	Type	H_w (mm)	L_w (mm)	t_w (mm)	b_b (mm)	h_b (mm)	P_h (%)	P_v (%)	P_{be} (%)	f'_c (MPa)	f_{yh} (MPa)	f_{yv} (MPa)	f_{ybe} (MPa)	$N/(A_w f'_c)$	V_{exp} (kN)
1	2	RC-M-1.2	Rect w/B	1200	1000	100	100	150	0.63	0.63	3.54	46	667	667	484	0	345
2	2	RC-H-1.2	Rect w/B	1200	1000	100	100	150	0.86	0.86	6.46	46	633	633	472	0	465
3	2	RC-M-1.5	Rect w/B	1500	1000	100	100	150	0.63	0.63	6.46	47	667	667	472	0	350
4	2	RC-H-1.5	Rect w/B	1500	1000	100	100	150	0.69	0.69	8.85	42	622	622	478	0	530
5	3	NS1M	Rect w/B	1750	1500	200	200	300	0.93	1.1	9.57	53	470	470	617	0.07	2275
6	3	HS1M	Rect w/B	1750	1500	200	200	300	0.68	0.7	9.57	53	667	667	617	0.07	2111
7	3	NS0.5M	Rect w/B	1000	1500	200	200	100	0.93	0.92	9.62	45	470	617	617	0.07	2492
8	3	HS0.5M	Rect w/B	1000	1500	200	200	100	0.68	0.58	9.62	37	667	617	617	0.07	2351
9	7	PW1	Rect w/B	4691	3048	152	152	305	0.28	0.28	3.5	36	522	579	579	0.1	836
10	7	PW2	Rect w/B	4691	3048	152	152	305	0.28	0.28	3.5	40	522	579	579	0.13	1228
11	7	PW3	Rect w/B	4691	3048	152	152	305	0.28	1.57	2	34	522	353	353	0.1	1005
12	7	PW4	Rect w/B	4691	3048	152	152	305	0.28	0.28	3.5	29	522	462	462	0.12	970
13	8	SW-7	Rect w/B	1905	1905	76	76	191	0.27	0	8.19	43	414	448	448	0	519
14	8	SW-8	Rect w/B	1905	1905	76	76	191	0.27	0	8.19	42	465	448	448	0	569
15	9	MCN50M	Rect w/B	2498.08	2402	102	102	240	0.14	0.14	3.27	19	447	447	434	0.01	408
16	9	MCN100M	Rect w/B	2498.08	2402	101	101	240	0.28	0.28	4.68	19	447	447	430	0.01	617
17	9	MCN50C	Rect w/B	2494.96	2399	102	102	240	0.14	0.14	3.27	18	447	447	434	0.01	352
18	9	MCN100C	Rect w/B	2492.88	2397	101	101	240	0.28	0.28	4.69	18	447	447	430	0.01	453
19	9	MRN100C	Rect w/B	2484	5400	100	100	200	0.28	0.28	2.84	16	447	447	443	0.02	766
20	9	MRN50mC	Rect w/B	2482.16	5396	103	103	200	0.12	0.12	2.91	20	605	605	456	0.01	776
21	9	MCN50mC	Rect w/B	2493.92	2398	103	103	240	0.12	0.12	3.45	20	605	605	443	0.01	329
22	9	MEN50mC	Rect w/B	2502.78	1239	101	101	124	0.12	0.12	4.54	20	605	605	443	0.01	154
23	9	MCN50mD	Rect w/B	2318.36	1916	83	83	192	0.11	0.11	3.77	25	630	630	411	0.01	234
24	9	MCN100D	Rect w/B	2324.41	1921	84	84	192	0.26	0.26	4.96	25	435	435	411	0.01	274
25	10	S4-Z4B2-1	Rect w/B	2250	2000	200	200	300	0.25	0.57	1.34	39	327	495	488	0.4	1104
26	10	S4-Z4B2-2	Rect w/B	2250	2000	200	200	300	0.25	0.57	1.34	39	327	495	488	0.4	1083
27	10	S5-Z4B2-1	Rect w/B	2250	2000	200	200	300	0.25	0.7	1.34	39	327	465	488	0.4	1140
28	10	S5-Z4B2-2	Rect w/B	2250	2000	200	200	300	0.25	0.7	1.34	39	327	465	488	0.4	1166
29	11	M60	Rect w/B	2159	2032	203	203	254	0.34	0.34	4.04	39	453	453	440	0	1122
30	11	M115	Rect w/B	2159	2032	203	203	254	0.17	0.17	2.33	38	786	786	770	0	1104
31	11	H60	Rect w/B	2159	2032	203	203	254	0.86	0.86	6.63	44	475	475	450	0	1969
32	11	H115	Rect w/B	2159	2032	203	203	254	0.43	0.43	3.51	44	806	806	770	0	1808
33	11	H60X	Rect w/B	2159	2032	203	203	254	0.86	0.86	6.63	42	475	475	450	0	1954
34	12	EB	Rect w/B	2159	2032	203	203	406	0.82	0.82	4.6	44.7	441	441	446	0	1680

No.	Ref.	Specimen ID	Type	H_w (mm)	L_w (mm)	t_w (mm)	b_b (mm)	h_b (mm)	P_h (%)	P_v (%)	P_{be} (%)	f'_c (MPa)	f_{yh} (MPa)	f_{yv} (MPa)	f_{ybe} (MPa)	$N/(A_w f'_c)$	V_{exp} (kN)
35	12	3B	Rect w/B	2159	2032	203	203	254	0.82	0.82	5.16	49.1	441	441	446	0	1950
36	14	W7	Rect w/B	1500	750	125	125	210	0.67	0.46	1.8	31	588	588	604	0	203
37	14	W9	Rect w/B	1500	750	125	125	75	0.2	1.05	2.41	31	588	604	604	0	177
38	14	W11	Rect w/B	1500	750	125	125	75	0.11	1.05	2.41	31	588	604	604	0	173
39	14	W13	Rect w/B	1500	750	125	125	75	0.11	1.05	2.41	25	588	604	604	0	158
40	24	6	Rect w/B	1801	1300	120	120	130	0.13	0.26	6.53	18	314	314	471	0	309
41	24	7	Rect w/B	1801	1300	120	120	130	0.25	0.13	6.53	18	471	471	471	0	364
42	24	8	Rect w/B	1801	1300	120	120	130	0.25	0.26	6.53	16	471	471	471	0	374
43	24	9	Rect w/B	1801	1300	100	100	130	0.26	0.26	7.01	18	366	366	471	0	258
44	24	10	Rect w/B	1801	1300	80	80	130	0.25	0.25	7.31	16	367	367	471	0	187
45	24	11	Rect w/B	1400	1400	100	100	140	0.13	0.26	5.71	16	362	362	471	0	235
46	24	12	Rect w/B	1400	1400	100	100	140	0.26	0.13	5.71	17	366	366	471	0	304
47	24	13	Rect w/B	1400	1400	100	100	140	0.26	0.26	5.71	18	370	370	471	0	289
48	24	14	Rect w/B	1199	1700	80	80	170	0.13	0.25	4.41	17	366	366	471	0	255
49	24	15	Rect w/B	1199	1700	80	80	170	0.25	0.13	4.41	19	366	366	471	0	368
50	24	16	Rect w/B	1199	1700	80	80	170	0.25	0.25	4.41	19	366	366	471	0	362
51	24	21	Rect w/B	1801	1300	100	100	130	0	0	4.62	24	0	0	471	0	258
52	24	22	Rect w/B	1801	1300	100	100	130	0	0	4.62	17	0	0	471	0	222
53	24	23	Rect w/B	1801	1300	100	100	130	0.25	0	8.54	24	431	431	471	0	333
54	24	24	Rect w/B	1801	1300	100	100	130	0	0.25	4.62	24	0	431	471	0	232
55	24	25	Rect w/B	1400	1400	100	100	140	0	0	4.29	24	0	0	471	0	352
56	24	26	Rect w/B	1400	1400	100	100	140	0	0	4.29	18	0	0	471	0	262
57	24	27	Rect w/B	1400	1400	100	100	140	0.25	0	6.5	24	431	0	471	0	491
58	24	28	Rect w/B	1400	1400	100	100	140	0	0.25	4.29	23	0	431	471	0	258
59	24	29	Rect w/B	1049	1501	80	80	150	0	0	5	23	0	0	471	0	400
60	24	30	Rect w/B	1049	1501	80	80	150	0	0	5	18	0	0	471	0	356
61	24	31	Rect w/B	1049	1501	80	80	150	0.25	0	6.67	23	431	0	471	0	391
62	24	32	Rect w/B	1049	1501	80	80	150	0	0.25	5	23	0	448	471	0	344
63	23	W2	Rect w/B	2000	1500	200	200	200	0.29	0.32	1.28	28	335	335	395	0.1	443
64	24	1	Rect w/B	2000	1000	120	120	100	0.13	0.25	8.5	19	392	392	471	0	198
65	24	2	Rect w/B	2000	1000	120	120	100	0.25	0.25	8.5	20	402	402	471	0	270
66	24	4	Rect w/B	2000	1000	120	120	100	0.38	0.25	10.57	20	402	402	471	0	324
67	25	72	Rect w/B	1700	1700	160	160	170	0.26	0.51	5.68	17	419	407	376	0.11	772
68	25	73	Rect w/B	1700	1700	160	160	170	0.26	0.51	5.68	21	419	407	376	0.09	775
69	25	74	Rect w/B	1700	1700	160	160	170	0.57	0.51	5.68	21	421	407	376	0.09	790
70	25	75	Rect w/B	1700	1700	160	160	170	0.57	0.51	5.68	14	421	407	376	0.14	812
71	25	76	Rect w/B	1700	1700	160	160	170	1.08	0.51	5.68	15	415	407	376	0.13	794
72	25	77	Rect w/B	1700	1700	160	160	170	1.08	0.51	5.68	18	415	407	376	0.11	875
73	25	78	Rect w/B	1700	1700	160	160	170	0.61	0.51	2.51	21	421	407	382	0.09	662
74	25	79	Rect w/B	1700	1700	160	160	170	0.61	0.51	2.51	14	421	407	382	0.14	591

No.	Ref.	Specimen ID	Type	H_w (mm)	L_w (mm)	t_w (mm)	b_b (mm)	h_b (mm)	P_h (%)	P_v (%)	P_{be} (%)	f'_c (MPa)	f_{yh} (MPa)	f_{yv} (MPa)	f_{ybe} (MPa)	$N/(A_w f'_c)$	V_{exp} (kN)
75	25	80	Rect w/B	1700	1700	160	160	170	1.08	0.51	2.51	15	415	407	382	0.13	657
76	25	81	Rect w/B	1700	1700	160	160	170	1.08	0.51	2.51	18	415	407	382	0.11	713
77	25	82	Rect w/B	1700	850	160	160	85	0.57	0.4	9.91	21	421	407	381	0.09	318
78	25	83	Rect w/B	1700	850	160	160	85	0.57	0.4	9.91	18	421	407	381	0.11	304
79	25	84	Rect w/B	1700	850	160	160	85	1.08	0.4	8.44	18	415	407	378	0.11	319
80	25	85	Rect w/B	1700	850	160	160	85	1.08	0.4	8.44	21	415	407	378	0.09	336
81	25	Ohono_1-1	Rect w/B	400	900	100	100	90	0.1	0.1	5	30	224	224	224	0	254
82	25	Ohono_1-2	Rect w/B	400	900	100	100	90	0.1	0.1	5	29	224	224	224	0	204
83	25	Yoshizaki-165	Rect w/B	860	800	60	60	86	0.23	0.22	4.92	24	433	433	333	0	102
84	25	Yoshizaki-166	Rect w/B	860	800	60	60	86	0.82	0.73	5.47	24	433	433	343	0	147
85	25	Yoshizaki-167	Rect w/B	860	800	60	60	86	0.41	0.44	7.71	24	433	433	343	0	135
86	25	Yoshizaki-168	Rect w/B	860	800	60	60	86	0.82	0.73	8.25	24	433	433	345	0	159
87	25	Yoshizaki-169	Rect w/B	860	800	60	60	86	1.17	1.17	8.25	24	433	433	345	0	175
88	25	Yoshizaki-170	Rect w/B	860	1200	60	60	120	0.23	0.24	3.52	25	433	433	333	0	160
89	25	Yoshizaki-171	Rect w/B	860	1200	60	60	120	0.82	0.78	3.91	25	433	433	343	0	235
90	25	Yoshizaki-172	Rect w/B	860	1200	60	60	120	0.41	0.44	5.52	25	433	433	343	0	220
91	25	Yoshizaki-173	Rect w/B	860	1200	60	60	120	0.82	0.78	5.91	25	433	433	345	0	269
92	25	Yoshizaki-174	Rect w/B	860	1200	60	60	120	1.17	1.17	5.91	25	433	433	345	0	275
93	25	Yoshizaki-175	Rect w/B	860	1200	60	60	120	0.23	0.22	3.53	26	433	433	433	0	199
94	25	Yoshizaki-176	Rect w/B	860	1600	60	60	160	0.82	0.8	2.94	26	433	433	343	0	322
95	25	Yoshizaki-177	Rect w/B	860	1600	60	60	160	0.41	0.37	4.44	26	433	433	345	0	279
96	25	Yoshizaki-178	Rect w/B	860	1600	60	60	160	0.82	0.8	4.44	26	433	433	345	0	382
97	25	Yoshizaki-179	Rect w/B	860	1600	60	60	160	1.17	1.17	4.73	26	433	433	351	0	422
98	26	WSL1	Rect w/B	1750	1600	100	100	300	0.2	0.2	4.02	29	604	604	438	0	349
99	26	WSL2	Rect w/B	1750	1600	100	100	300	0.2	0.2	1.34	29	604	604	438	0	233
100	26	WSL3	Rect w/B	1750	1600	100	100	300	0.26	0.26	4.02	29	601	601	438	0	471
101	26	WSL4	Rect w/B	1750	1600	100	100	300	0.14	0.14	4.02	29	632	632	438	0	403
102	26	WSL5	Rect w/B	1750	1600	100	100	300	0.2	0.2	4.02	29	446	446	438	0	357
103	26	WSL6	Rect w/B	1750	1600	100	100	300	0.14	0.14	4.02	29	446	446	438	0	416
104	26	WSL7	Rect w/B	1750	1600	80	80	300	0.68	0.25	3.35	29	604	604	438	0	324
105	26	WSL8	Rect w/B	1750	1600	80	80	300	0.48	0.17	3.35	29	632	632	438	0	292
106	26	WSL9	Rect w/B	1750	1600	80	80	300	0.25	0.25	3.35	29	446	446	438	0	336
107	28	C1.0	Rect w/B	1350	1200	100	100	210	0.84	0.32	2.24	35	520	520	520	0.07	455
108	28	C1.5	Rect w/B	1950	1200	100	100	210	0.84	0.32	2.24	34	520	520	520	0.07	304
109	29	SW11	Rect w/B	825	750	70	70	140	1.1	2.4	3.1	42	520	470	470	0	260
110	29	SW12	Rect w/B	825	750	70	70	140	1.1	2.4	3.1	43	520	470	470	0.1	340
111	29	SW13	Rect w/B	825	750	70	70	140	1.1	2.4	3.1	32	520	470	470	0.2	330
112	29	SW14	Rect w/B	825	750	70	70	140	1.1	2.4	3.1	34	520	470	470	0	265
113	29	SW15	Rect w/B	825	750	70	70	140	1.1	2.4	3.1	35	520	470	470	0.1	320
114	29	SW16	Rect w/B	825	750	70	70	140	1.1	2.4	3.1	41	520	470	470	0.2	355

No.	Ref.	Specimen ID	Type	H_w (mm)	L_w (mm)	t_w (mm)	b_b (mm)	h_b (mm)	P_h (%)	P_v (%)	P_{be} (%)	f'_c (MPa)	f_{yh} (MPa)	f_{yv} (MPa)	f_{ybe} (MPa)	$N/(A_w f'_c)$	V_{exp} (kN)
115	29	SW17	Rect w/B	825	750	70	70	140	1.1	2.4	3.1	39	520	470	470	0	247
116	29	SW21	Rect w/B	1375	650	65	65	140	0.8	2.5	3.3	34	520	470	470	0	127
117	29	SW22	Rect w/B	1375	650	65	65	140	0.8	2.5	3.3	40	520	470	470	0.1	150
118	29	SW23	Rect w/B	1375	650	65	65	140	0.8	2.5	3.3	38	520	470	470	0.2	180
119	29	SW24	Rect w/B	1375	650	65	65	140	0.8	2.5	3.3	39	520	470	470	0	120
120	29	SW25	Rect w/B	1375	650	65	65	140	0.8	2.5	3.3	36	520	470	470	0.2	150
121	29	SW26	Rect w/B	1375	650	65	65	140	0.8	2.5	3.3	24	520	470	470	0	123
122	30	SW31	Rect w/B	1375	650	65	65	140	0.35	1.5	3.3	28	520	470	470	0	116
123	30	SW32	Rect w/B	1375	650	65	65	140	0.35	1.5	3.3	43	520	470	470	0	111
124	30	SW32R	Rect w/B	1375	650	65	65	140	0.35	1.5	3.3	31	520	470	470	0	83
125	30	SW33	Rect w/B	1375	650	65	65	140	0.35	1.5	3.3	39	520	470	470	0	112
126	30	SW33R	Rect w/B	1375	650	65	65	140	0.35	1.5	3.3	30	520	470	470	0	94

APPENDIX-B

No.	V_{exp}	Dr. Azam Khan's Model	ASCE-43	EN-1998	Gulec Whittaker	Proposed Model	Wood et al	Barda et al	ACI 18.10.4
1	345	333.0	419.5	672.6	533.0	307.4	339.1164992	422.226836	562.9333886
2	465	476.0	543.7	1003.9	541.5	416.1	339.1164992	496.728836	562.9333886
3	350	333.2	418.9	1193.4	612.8	336.3	342.78273	398.151443	569.0193318
4	530	562.6	427.9	1092.7	555.4	366.6	324.0370349	395.547777	537.901478
5	2275	2485.9	2778.1	2250.0	2284.0	1873.6	2221	1654.47841	1812.747362
6	2111	2171.7	2286.4	2100.0	2282.3	1856.2	2018	1564.29841	1812.747362
7	2492	2511.0	2844.9	2100.0	2431.0	2445.0	2445	1803.46466	1670.342779
8	2351	2200.0	2400.0	2231.0	2112.0	1566.1	2312	1340.99355	1514.60787
9	836	808.0	1126.1	767.0	805.5	819.0	866	1279.25489	1354.723834
10	1228	1311.0	1321.0	1222.0	1019.2	845.5	1255	1421.73402	1391.375347
11	1005	1090.0	976.1	1044.0	761.3	813.5	1350.728345	1101	1335.633502
12	970	925.0	933.0	890.0	709.1	681.1	1247.462657	1120.57816	1285.291479
13	519	522.0	960.5	620.0	488.5	418.9	474.6929748	262.030522	399.1815714
14	569	570.0	600.4	555.0	477.3	417.2	469.1408192	258.965732	416.3416996
15	408	404.0	497.9	401.0	380.2	322.7	533.9738384	388.347818	420.3104224
16	617	763.7	624.2	642.0	382.3	419.5	528.7388008	475.632686	568.0100636
17	352	347.0	498.0	346.0	359.6	316.5	519.0828454	379.787427	412.6734311
18	453	466.0	465.0	476.0	361.0	411.1	513.5652912	466.653085	559.7912508
19	766	864.0	878.7	734.1	755.0	756.4	1080	1174.5648	1215.864
20	776	855.0	802.9	928.3	810.0	750.3	1242.779749	1113.90678	1024.891963
21	329	335.0	361.3	333.0	345.0	350.5	552.295374	414.300315	455.465331
22	154	-35.2	142.0	144.0	497.1	123.4	279.8193106	140.800222	185.9894796
23	234	224.1	274.7	222.0	244.0	216.8	397.57	270.506628	308.991404
24	274	237.5	562.4	276.0	288.0	272.5	403.41	316.886623	384.207684
25	1104	1204.0	1460.8	1149.0	769.8	716.6	1248.9996	1121	951.4997998
26	1083	1101.0	1144.0	1149.0	769.8	716.6	1248.9996	1020	951.4997998
27	1140	1201.0	1747.6	1149.0	770.0	744.6	1248.9996	1246	951.4997998
28	1166	1188.0	1234.0	1149.0	770.0	744.6	1248.9996	1156	951.4997998
29	1122	1300.0	1381.6	1138.3	1131.0	949.1	1288.018347	1071.89564	1279.335513
30	1104	1098.0	1198.0	1114.4	1121.0	922.9	1271.398059	1012.4935	1186.876185
31	1969	1921.0	2040.1	1567.3	2005.1	1558.4	1878	1744.66835	2271.036803
32	1808	1712.0	2076.5	1567.3	1996.9	1428.5	1368.09446	1591.41784	2113.675867
33	1954	1851.0	2003.0	1510.6	1917.4	1537.5	2116	1727.80079	2218.822081
34	1680	1777.0	2166.7	1553.9	1515.0	1501.0	1702	1634.45423	2181.135079

No.	V_{exp}	Dr. Azam Khan's Model	ASCE-43	EN-1998	Gulec Whittaker	Proposed Model	Wood et al	Barda et al	ACI 18.10.4
35	1950	2102.0	2166.6	1705.6	2213.5	1391.4	2088	1669.99385	2214.27226
36	203	380.7	392.1	210.0	265.6	172.8	260.9889545	230.441686	433.2416645
37	177	435.9	118.9	138.9	266.5	183.8	297.28125	435.034186	198.9862445
38	173	471.9	258.0	138.9	266.5	178.3	297.28125	435.034186	149.3737445
39	158	428.0	258.8	115.1	217.3	173.8	297.28125	427.05	140.325
40	309	404.0	179.0	293.9	386.2	228.2	330.9259736	226.947665	229.1421868
41	364	365.0	442.2	293.9	385.8	235.9	330.9259736	207.843905	349.1529868
42	374	377.0	470.4	263.5	346.0	239.7	312	256.54608	339.69
43	258	287.0	566.5	244.9	384.5	206.2	275.7716447	199.668654	261.5938223
44	187	223.7	273.2	175.7	340.8	157.3	208	151.86768	199.42
45	235	189.0	211.0	181.0	339.0	235.3	280	233.6208	205.884
46	304	401.0	213.3	191.4	358.5	238.6	288.6173938	199.284001	277.5326969
47	289	292.0	287.8	201.8	379.4	257.1	296.9848481	244.743636	283.172424
48	255	267.0	247.7	125.5	439.2	265.5	280.3711825	250.250906	204.8943913
49	368	377.0	170.0	386.3	488.7	276.3	296.4051282	224.453699	272.6425641
50	362	382.0	274.7	386.3	489.2	286.5	296.4051282	260.292419	272.6425641
51	258	174.0	244.0	883.7	267.0	159.6	318.4336666	144.850086	159.2168333
52	222	190.9	233.0	645.3	357.7	137.0	268.0018657	121.909513	134.0009328
53	333	186.9	94.5	883.7	509.1	234.1	318.4336666	144.850086	299.2918333
54	232	184.3	11.5	883.7	502.9	183.5	318.4336666	228.895086	159.2168333
55	352	197.6	340.0	728.2	495.6	218.2	342.928564	189.296567	171.464282
56	262	282.0	265.0	560.6	374.4	191.7	296.9848481	163.935636	148.492424
57	491	512.0	521.0	728.2	501.2	286.9	342.928564	189.296567	322.314282
58	258	277.0	240.0	700.9	477.0	240.1	335.7082066	275.82093	167.8541033
59	400	733.3	421.0	392.9	459.4	261.2	287.9417247	180.794408	143.9708623
60	356	366.0	340.0	314.3	362.4	229.4	254.7281469	159.940087	127.3640734
61	391	421.0	450.0	392.9	463.8	311.5	287.9417247	180.794408	273.3570623
62	344	365.0	89.8	392.9	460.6	284.2	287.9417247	261.488168	143.9708623
63	443	451.0	98.0	450.0	451.0	300.2	455	690.423484	688.3126967
64	198	347.7	49.4	787.6	291.7	155.3	261.5339366	149.020181	150.0735384
65	270	361.2	98.9	825.5	306.3	166.1	268.3281573	152.858447	211.8315735
66	324	656.2	151.2	825.5	309.5	185.5	268.3281573	152.858447	274.5435735
67	772	731.0	733.0	1055.1	777.0	557.1	773	724.580026	576.6879825
68	775	788.0	766.0	1280.9	781.0	587.1	799	759.889363	607.9319473
69	790	789.0	865.0	1280.9	784.0	626.3	767	759.889363	964.3335473
70	812	814.0	904.0	880.1	955.8	573.1	508.8654046	699.615943	844.7165716
71	794	821.0	806.0	938.9	983.0	644.0	526.7257351	709.066846	874.3647202
72	875	877.0	877.0	1112.3	888.0	669.1	898	738.041762	957.8185615
73	662	589.0	605.0	1280.9	675.0	454.9	623.2302945	759.889363	1010.138347
74	591	633.0	580.0	880.1	943.5	428.8	508.8654046	699.615943	844.7165716

No.	V_{exp}	Dr. Azam Khan's Model	ASCE-43	EN-1998	Gulec Whittaker	Proposed Model	Wood et al	Barda et al	ACI 18.10.4
75	657	688.0	655.0	938.9	970.6	490.3	526.7257351	709.066846	874.3647202
76	713	750.0	323.4	1112.3	733.0	502.4	576.9991334	738.041762	957.8185615
77	318	311.4	230.4	964.0	412.4	243.9	311.6151473	264.885344	432.3083501
78	304	297.4	230.6	837.1	389.2	235.7	288.4995667	259.78667	424.4490527
79	319	367.4	438.2	837.1	387.0	253.3	288.4995667	259.78667	478.9092808
80	336	391.8	438.1	964.0	410.3	260.3	311.6151473	264.885344	517.2811444
81	254	516.3	244.0	141.5	172.9	213.9	246.4751509	182.656804	143.3975754
82	204	517.9	200.0	137.4	167.3	211.0	242.3324163	179.790032	141.3262082
83	102	232.6	97.3	245.3	167.7	78.2	117.5755077	90.1143831	106.5909538
84	147	-15.2	338.1	245.3	169.3	114.7	117.5755077	153.713423	195.1753427
85	135	-4.8	182.6	245.3	170.2	108.9	117.5755077	117.549263	144.0021538
86	159	45.5	338.1	245.3	171.2	131.6	117.5755077	153.713423	195.1753427
87	175	102.3	506.3	245.3	172.2	155.1	117.5755077	208.583183	195.1753427
88	160	427.0	103.1	252.2	318.5	131.0	180	157.10544	161.7048
89	235	616.2	341.6	252.2	320.5	188.7	180	258.11568	298.8
90	220	145.0	187.8	252.2	321.4	181.0	180	194.51664	217.8216
91	269	203.6	341.6	252.2	322.8	218.8	180	258.11568	298.8
92	275	253.1	506.8	252.2	323.9	251.6	180	331.06752	298.8
93	199	112.6	96.3	261.1	332.2	149.6	183.5647025	155.586556	163.4871512
94	322	404.4	347.1	235.9	510.4	266.6	244.7529367	363.155976	406.2898748
95	279	382.8	161.2	235.9	511.7	260.0	244.7529367	255.910536	292.8052683
96	382	412.2	347.1	235.9	513.1	309.3	244.7529367	363.155976	406.2898748
97	422	438.5	507.0	235.9	514.9	360.6	244.7529367	455.436936	406.2898748
98	349	356.0	120.3	318.1	410.8	362.2	430.8131846	343.598916	408.6865923
99	233	321.0	120.3	318.1	404.3	228.5	430.8131846	343.598916	408.6865923
100	471	420.0	155.8	318.1	411.1	377.2	430.8131846	377.640516	465.4225923
101	403	444.0	88.0	318.1	410.5	348.6	430.8131846	312.571716	356.9745923
102	357	331.0	88.7	318.1	410.5	348.9	430.8131846	313.262916	358.1265923
103	416	441.0	61.9	318.1	410.3	337.6	430.8131846	287.573316	315.3105923
104	324	386.0	304.8	254.5	407.5	315.4	344.6505477	298.072733	572.1199091
105	292	301.0	223.3	254.5	407.2	291.7	344.6505477	264.618653	560.6260738
106	336	301.0	111.0	254.5	407.3	265.5	344.6505477	267.736733	315.0452738
107	455	476.0	334.9	279.0	449.6	294.8	354.964787	348.667172	589.2415464
108	304	324.0	435.5	345.8	311.0	233.8	349.8571137	300.666631	580.7628087
109	260	384.7	761.0	426.2	267.0	232.7	170.1194433	444.938923	282.3982759
110	340	344.3	761.0	434.3	501.7	243.5	172.1327613	479.862039	285.7403837
111	330	416.6	761.1	340.4	546.6	239.1	162.855	483.945809	246.4974239
112	265	497.3	761.0	358.3	218.3	223.7	162.855	435.953318	254.0837288
113	320	467.2	761.0	367.1	410.6	235.3	162.855	464.693009	257.7931765
114	355	481.6	761.0	418.1	697.0	248.4	168.0820112	508.440604	279.0161386

No.	V_{exp}	Dr. Azam Khan's Model	ASCE-43	EN-1998	Gulec Whittaker	Proposed Model	Wood et al	Barda et al	ACI 18.10.4
115	247	441.9	761.0	200.7	248.7	229.5	163.9311975	441.678955	272.1257878
116	127	301.7	186.9	205.9	226.5	141.3	204.4769056	331.234495	204.4769056
117	150	359.6	186.8	235.5	486.1	149.6	221.7863437	359.409511	221.1861186
118	180	348.6	186.9	225.9	188.0	152.1	216.170588	381.307982	216.170588
119	120	223.2	186.8	230.7	258.1	144.1	218.9964673	333.604185	218.9964673
120	150	337.9	186.9	216.0	157.0	151.1	210.405	377.832	210.405
121	123	334.4	187.1	152.1	163.1	134.1	171.7949631	325.900584	171.7949631
122	116	267.4	162.5	174.3	185.5	96.8	157.5234375	209.002092	114.9012176
123	111	121.0	162.0	249.6	119.0	105.6	157.5234375	216.24736	123.9938022
124	83	78.0	162.4	380.7	97.0	98.9	157.5234375	210.583207	116.8854675
125	112	102.0	162.1	121.0	124.0	103.6	157.5234375	214.459185	121.7496981
126	94	85.0	162.4	111.0	103.0	98.2	157.5234375	210.065031	116.2351727